MARTIN MARIETTA ENERGY SYSTEMS LIBRARIES
3 4456 0361038 6

CENTRAL RESEARCH LIBRARY
DOCUMENT COLLECTION

6

ORNL-2152
Reactors – General

HRP RADIATION CORROSION STUDIES:

IN-PILE LOOP L-4-11

J. R. McWherter
J. E. Baker

OAK RIDGE NATIONAL LABORATORY
operated by
UNION CARBIDE CORPORATION
for the
U.S. ATOMIC ENERGY COMMISSION

CENTRAL RESEARCH LIBRARY
DOCUMENT COLLECTION
LIBRARY LOAN COPY
DO NOT TRANSFER TO ANOTHER PERSON
If you wish someone else to see this document, send in name with document and the library will arrange a loan.

Printed in USA. Price 1.50 cents. Available from the

Office of Technical Services
U. S. Department of Commerce
Washington 25, D. C.

LEGAL NOTICE

This report was prepared as an account of Government sponsored work. Neither the United States, nor the Commission, nor any person acting on behalf of the Commission:

A. Makes any warranty or representation, express or implied, with respect to the accuracy, completeness, or usefulness of the information contained in this report, or that the use of any information, apparatus, method, or process disclosed in this report may not infringe privately owned rights; or

B. Assumes any liabilities with respect to the use of, or for damages resulting from the use of any information, apparatus, method, or process disclosed in this report.

As used in the above, "person acting on behalf of the Commission" includes any employee or contractor of the Commission to the extent that such employee or contractor prepares, handles or distributes, or provides access to, any information pursuant to his employment or contract with the Commission.

ORNL-2152
Reactors – General
TID-4500 (13th ed. Rev.)
February 15, 1958

Contract No. W-7405-eng-26

REACTOR EXPERIMENTAL ENGINEERING DIVISION

HRP RADIATION CORROSION STUDIES:

IN-PILE LOOP L-4-11

J. R. McWherter
J. E. Baker

Other contributors to this report:

E. G. Bohlmann
N. C. Bradley
G. H. Jenks
D. T. Jones
A. R. Olsen
M. L. Picklesimer
H. C. Savage
F. J. Walter

DATE ISSUED

JUN 11 1958

OAK RIDGE NATIONAL LABORATORY
Oak Ridge, Tennessee
operated by
UNION CARBIDE CORPORATION
for the
U.S. ATOMIC ENERGY COMMISSION

MARTIN MARIETTA ENERGY SYSTEMS LIBRARIES

3 4456 0361038 6

CONTENTS

SUMMARY 1

INTRODUCTION 1

EQUIPMENT AND CONSTRUCTION 1

OPERATION AND PROCEDURES 5

- General Operating Conditions 5
- Out-of-Pile Pretreatment and Operation 6
- In-Pile Operation 6
- Dismantling 15

RESULTS 15

- Oxygen Consumption Data 15
- Solution Analyses 15
- Free Acid Concentration 20
- Uranium Balance 20
- Neutron Flux, Fission Power, and Gamma Heat 21
- Radiolytic Gas Pressure 24
- Qualitative Inspection of Loop 25
- Quantitative Inspection of Loop 38
  - Zirconium and Zirconium Alloys 38
  - Titanium Alloys 39
  - Stainless Steel 41
  - Incoloy 41
  - Platinum 42
  - Sintered Alumina 42
  - Synthetic Sapphire 42
- Metallographic Examination of Loop 42

DISCUSSION OF RESULTS 43

- Correlation Between Nickel, Manganese, Oxygen, and Weight Data 43
- Correlation Between Excess Acid and Over-All Rate 44
- Quantitative Weight Data 45
- Solution Stability 45
- Metallographic Results 45

HRP RADIATION CORROSION STUDIES: IN-PILE LOOP L-4-11

SUMMARY

The sixth in-pile loop experiment, L-4-11, was completed. The loop operated in-pile for a total of 1109 hr, during which time the LITR energy output was 2175 Mwhr. The main-stream operating temperature was 250°C. During this run the loop was drained and then recharged with fresh solution. Based on oxygen data, the corrosion rate for the first 110 hr of operation was 5.0 mpy; for the next 232 hr the rate was 1.7 mpy. For the first 120 hr of operation with the second fuel solution the corrosion rate was 7.2 mpy, and for the remainder of the run the rate was 1.9 mpy. The nickel data gave parallel results.

Corrosion specimens of a large variety of zirconium alloys, titanium alloys, and stainless steels, as well as specimens of synthetic sapphire, sintered alumina, platinum, and Incoloy, were included in the experiment. Corrosion rates of most of the zirconium alloys, titanium alloys, and stainless steels were generally consistent with rates observed in the previous in-pile loops.

The zirconium alloys Zr-3 (3% Ag), Zr-3 (0.52% Sn, 5.71% Ti, 40 ppm N_2), Zr-3 (0.52% Sn, 0.28% Fe, 5.66% Ti, 60 ppm N_2), Zr-3 (1.4% Fe), and Zr-4 (0.7% Fe, 2.8% Cr) corroded at rates about two to three times those observed for Zircaloy-2 at the same power density. The zirconium alloy containing 3.84% Al and 2.5% Mn corroded at rates about 10 to 20 times those for Zircaloy-2. The zirconium alloy containing 2% niobium corroded at the same rate as Zircaloy-2 in the core but at a much higher rate, 17 mpy, in the in-line position. However, a zirconium alloy containing 15% niobium corroded at less than one-third the Zircaloy-2 corrosion rates in the core and exhibited rates similar to Zircaloy-2 in the in-line position. Corrosion rates for Incoloy were found to be about the same as those for stainless steel exposed to similar conditions. All sintered aluminum oxide specimens in the main stream disintegrated; however, the aluminum oxide bearings in the low temperature region of the pump showed no measurable wear. Synthetic sapphire became claudy and corroded at a rate of 12 mpy. Platinum was slightly affected in the core.

INTRODUCTION

Loop L-4-11 is the sixth completed in-pile loop experiment. This experiment was inserted in the HB-4 hole at the LITR on October 21, 1955, and removed on December 12, 1955.

The purpose of this experiment was to compare the performance of a large number of materials under similar irradiation and exposure conditions.

EQUIPMENT AND CONSTRUCTION

The equipment employed in this experiment was similar in most respects to that used in the previous in-pile loop experiments.[1-6] A schematic drawing of the loop package is shown in Fig. 1.

The loop was constructed of type 347 stainless steel. A tabulation of the specimens in this loop is given in Tables 1–3. Inclusion of a large variety of test materials in this loop necessitated the adoption of a code for identification purposes.

Loop volumes and other specifications are given in Table 4; the sample loading is given in Table 5. Coupon specimens, ½ × ¼ × 0.06 in., in non-tapered Zircaloy-2 holders were located in both the core and in-line positions. This is the first in-pile loop in which non-tapered holders were used. The arrangement of the coupons in the holders is shown in

[1] G. H. Jenks *et al.*, *HRP Quar. Prog. Rep. Jan. 31, 1956*, ORNL-2057, p 92–96 (classified).

[2] J. E. Baker *et al.*, *HRP Radiation Corrosion Studies: In-Pile Loop L-4-8*, ORNL-2042 (Aug. 21, 1956).

[3] G. H. Jenks *et al.*, *HRP Quar. Prog. Rep. Jan. 31, 1955*, ORNL-1853, p 88–106.

[4] G. H. Jenks *et al.*, *HRP Quar. Prog. Rep. April 30, 1955*, ORNL-1895, p 99–118.

[5] G. H. Jenks *et al.*, *HRP Quar. Prog. Rep. July 31, 1955*, ORNL-1943, p 109–125 (classified).

[6] G. H. Jenks *et al.*, *HRP Quar. Prog. Rep. Oct. 31, 1955*, ORNL-2004, p 121–152 (classified).

Table 1. Sample Code and Specimen Materials: Zirconium and Zirconium Alloys

Code Letters	Alloy No.	Alloy	Description
Rod I		Zircaloy-3	0.7% Fe
Rod II		Zircaloy-3	1.4% Fe
Rod III		Zircaloy-3	3.5% Fe
Rod IV		Zircaloy-4	0.7% Fe, 2.8% Cr
WB		Zircaloy-2	cut from Newport News bottom weld
WC		Zircaloy-2	cut from Newport News weld
Z 50–57		Zircaloy-2	5 ppm H_2
Z 58–65		Zircaloy-2	500 ppm H_2
Z 66–73		Zircoloy-2	1000 ppm H_2
ZB		Zircaloy-2	Item #1157
ZC		Zircaloy-3	3% Ag
ZD	6	Zircaloy-3	0.26% Sn, 0.19% Fe, 40 ppm N_2
ZE	12A	Zircaloy-3	0.50% Sn, 0.44% Fe
ZF	13A	Zircaloy-3	0.50% Sn, 0.24% Fe, 0.25% Ni
ZG	19	Zircaloy-3	1.46% Sn, 0.25% Fe, 0.21% Mo, 50 ppm N_2
ZH 1–8		Zircaloy-2	1000 ppm H_2
ZH 9–16		Zircaloy-2	5 ppm H_2
ZH 17–24		Zircaloy-2	2000 ppm H_2
ZH 25–32		Zircaloy-2	3000 ppm H_2
ZI	32B	Zircaloy-3	0.47% Sn, 0.85% Fe, 0.78% Ni, 50 ppm N_2
ZJ	38	Zircaloy-3	0.56% Sn, 0.71% W, 60 ppm N_2
ZK	44	Zircaloy-3	0.52% Sn, 5.71% Ti, 40 ppm N_2
ZL	51	Zircaloy-3	0.52% Sn, 0.28% Fe, 5.66% Ti, 60 ppm N_2
ZM	57	Zircaloy-3	0.24% Fe, 0.32% Nb, 70 ppm N_2
ZN	61	Zircaloy-3	1.54% Sn, 0.26% Fe, 0.83% Nb, 80 ppm N_2
ZO	73	Zircaloy-3	3.84% Al, 2.5% Mn
ZP	70	Zircaloy-3	0.69% Sn, 0.69% Cu, 40 ppm N_2
ZQ		Zircaloy-3	0.81% Fe, 0.77% Cr
ZR		Zircaloy-3	0.72% Fe, 0.73% Cr, 0.45% Sn
ZS		Zircaloy-3	1.5% Cr, 0.50% Sn
ZT		Zircaloy-3	15% Nb; 500°C, 2 hr, *in vacuo*, slow cool
ZU		Zircaloy-3	2% Nb
ZZ		Crystal-bar zirconium	#1591-8

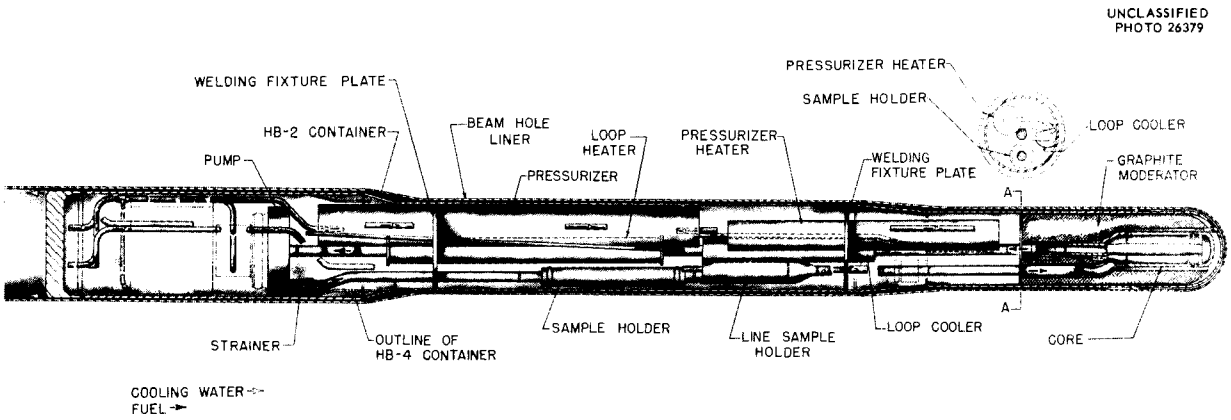

Fig. 1. LITR In-Pile Loop.

Table 2. Sample Code and Specimen Materials: Stainless Steel

Code Letters	Description
SA	SS 347, Item #1149
SE	SS 443, Lot #2, hot rolled ond annealed
SF	SS 446, Lot #2, rolled and pickled
SG	SS 350A, Item #381, as annealed

Table 3. Sample Code and Specimen Materials: Titanium

Code Letters	Description
TB	Ti-75A, Item #45
TD	Ti-110AT, Item #1176
TE	Ti-130AM, Item #1175

Table 4. Loop Volumes and Other Specifications

Loop volume (including pressurizer), ml	1540
Pressurizer volume, ml	559
Empty core volume, ml	370
Loaded core volume, ml	298
Flow rates	
Pressurizer, cc/sec	5.3
Core, gpm	7.3
In-line, gpm	7.3
Pump bearing material	Al_2O_3
Pump journal material	Al_2O_3
System pressure checked at, psi	1200
Minimum clearance for core and in-line holders	
Channel depth, in.	0.200
Channel width, in.	0.437

Fig. 2. Eight core rod coupon assemblies were installed in the core surrounding the core holder as shown in Fig. 3. Each assembly consisted of 11 corrosion coupon specimens, $\frac{1}{2} \times \frac{1}{2} \times 0.06$ in., mounted on type 347 stainless steel rods and separated by type 347 stainless steel tubular spacers. Each coupon had a 0.204-in.-dia hole drilled through its center through which the 0.200-in.-dia rod was passed. Arrangement of these specimens is shown in detail in Fig. 4. This loop also contained a special in-line specimen array consisting of four rod coupon assemblies as shown in Figs. 5 and 6. These assemblies were similar in construction and materials to those in the core but contained only ten coupons per rod. Both core and in-line rod coupon arrays contained zirconium alloys in the form of pins. The pins were 70 mils in diameter and 4 in. in length. Figs. 3 and 5 show the location of these pins.

Table 5. Corrosion Sample Units

Unit	Specimens
Core holder coupons	PT, Al_2O_3, ZZ, WB, TD, TE, ZD, ZE, ZF, ZG, ZI, ZJ, ZK, ZL, ZM, ZN, ZO, ZP, ZC, Z50, Z68, Incoloy, SE, SA
In-line holder coupons	PT, Al_2O_3, ZZ, WB, TD, TE, ZD, ZE, ZF, ZG, ZI, ZJ, ZK, ZL, ZM, ZN, ZO, ZP, ZC, Z50, Z68, Incoloy, SE, SA
Core rod coupons	ZT, PT, ZF, ZO, ZS, ZH, Al_2O_3, ZG, ZP, TB, SF, ZQ, ZZ, ZI, ZC, SG, ZR, WC, ZJ, ZU, TD, ZK, TE, ZL, Incoloy, ZD, ZM, SE, ZE, ZN, SA, ZR
Special in-line rod coupons	PT, TB, ZD, ZG, ZK, ZN, ZC, Incoloy, SA, TD, ZE, ZI, ZL, ZO, ZH, SE, ZZ, TE, ZF, ZJ, ZM, ZP, ZT, ZQ, ZR, ZS, SF, SG, ZU
Core pin specimens	Zircaloy-3, Zircaloy-4
Special in-line pin specimens	Zircaloy-3, Zircaloy-4
Special core specimens	Sapphire
Core and in-line holders	ZB

UNCLASSIFIED
ORNL—LR—DWG 27774

REAR FRONT

SA	SE	IN	Z-68	Z-50	ZC	ZP	ZO	ZN	ZM	ZL	ZK	ZJ	ZI	ZG	ZF	ZE	ZD	TE	TD	WB	ZZ	Al_2O_3	PT

Fig. 2. Arrangement of Coupon Corrosion Specimens in the Core Holder and in the In-Line Holder.

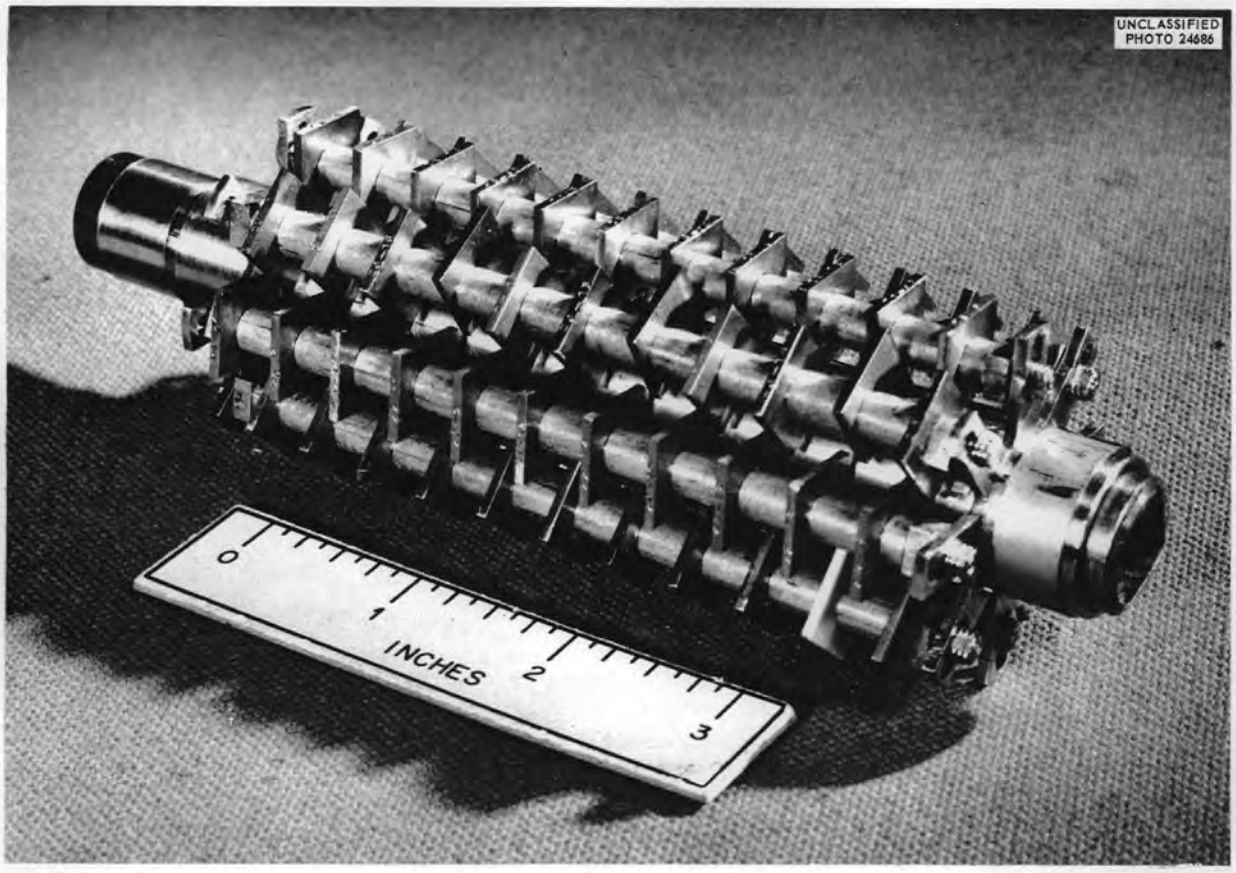

Fig. 3. Core Corrosion Specimen Assembly.

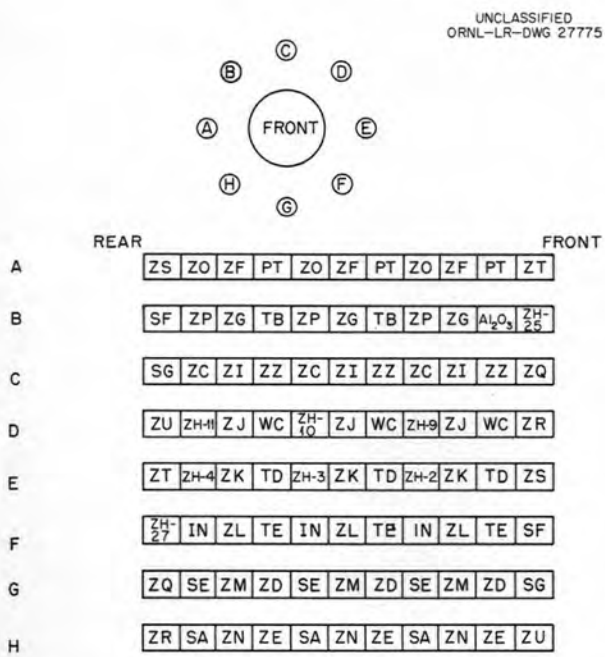

Fig. 4. Arrangement of Core Rod Coupon Assemblies.

Also included in the core were two specimens of sapphire mounted in special brackets located at the front end of the core holder. A photograph of these specimens taken prior to irradiation is shown in Fig. 7. This material is of interest for possible use as an insulator or as a transparent window.

The structure of the loop was essentially the same as that of the previous loops. The circulating pump was a modified ORNL 5-gpm model with pure sintered aluminum oxide bearings and journal bushings, identical to the one used in loop L-4-8 (ref 2).

OPERATION AND PROCEDURES

General Operating Conditions

The initial main-stream and pressurizer temperatures were 250°C and 280°C, respectively. These are the same as those that were used in previous loop experiments.

The original enriched solution charged to the loop was 0.17 *m* UO_2SO_4, 0.031 *m* $CuSO_4$, 0.04 *m*

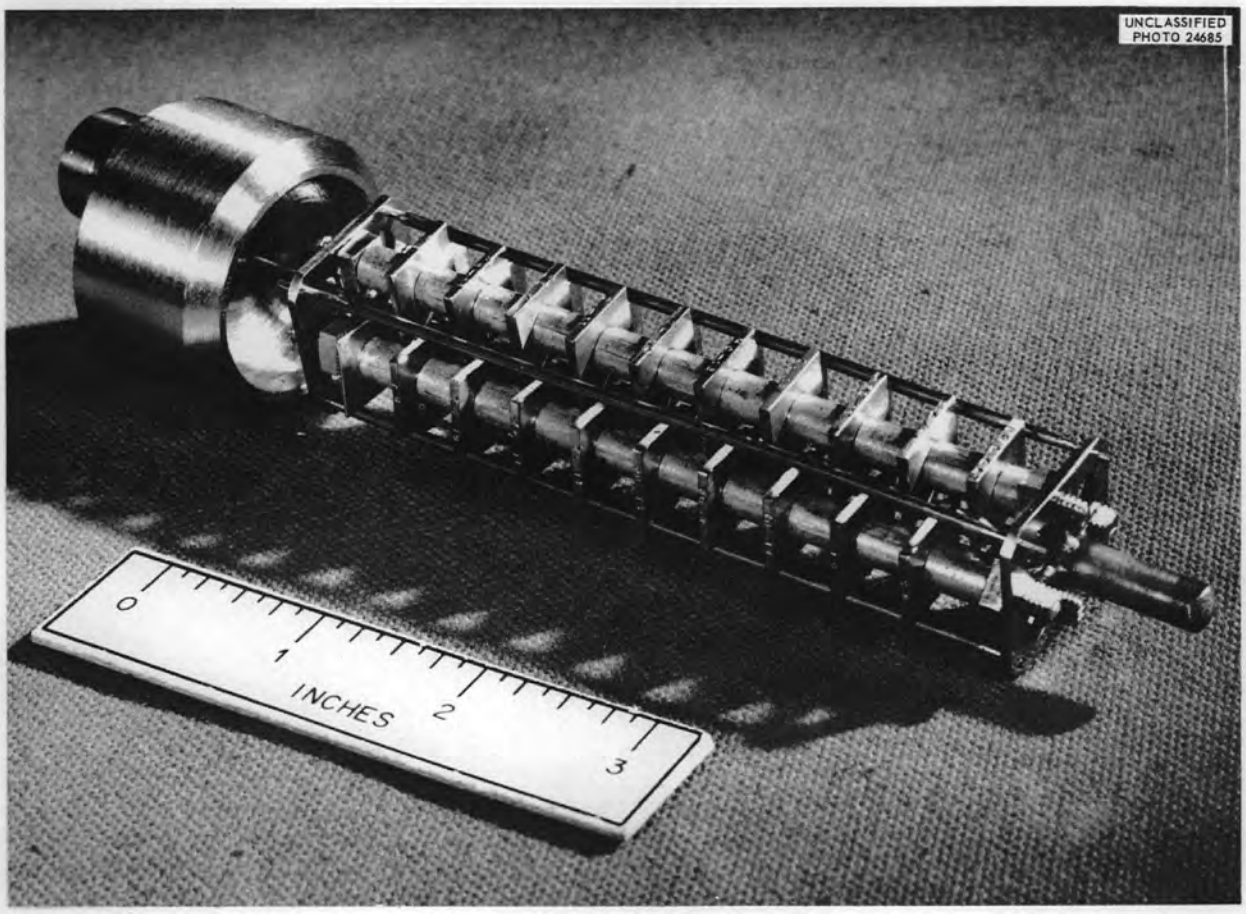

Fig. 5. Special In-Line Corrosion Specimen Assembly.

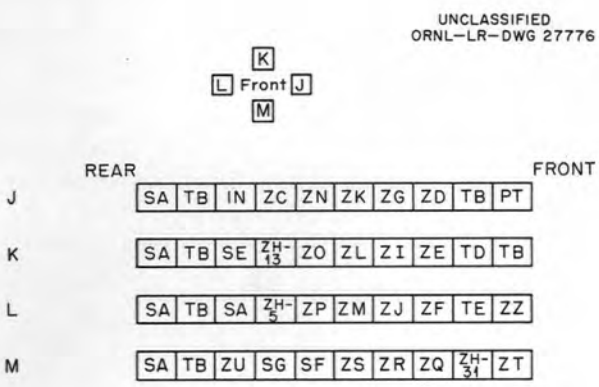

Fig. 6. Arrangement of Special In-Line Rod Coupons.

H_2SO_4, and 0.009 *m* $NiSO_4$. The oxygen partial pressure in the pressurizer was maintained between 42 and 140 psi, not including the oxygen from radiolytic gas formation.

Loop areas wetted by the circulating solution are shown in Tables 6–10.

Out-of-Pile Pretreatment and Operation

The loop preparatory operations and the results of solution analyses during these operations are summarized in Table 11.

In-Pile Operation

The loop was charged with the original enriched solution and operated at temperature about 22 hr before the reactor was taken to power.

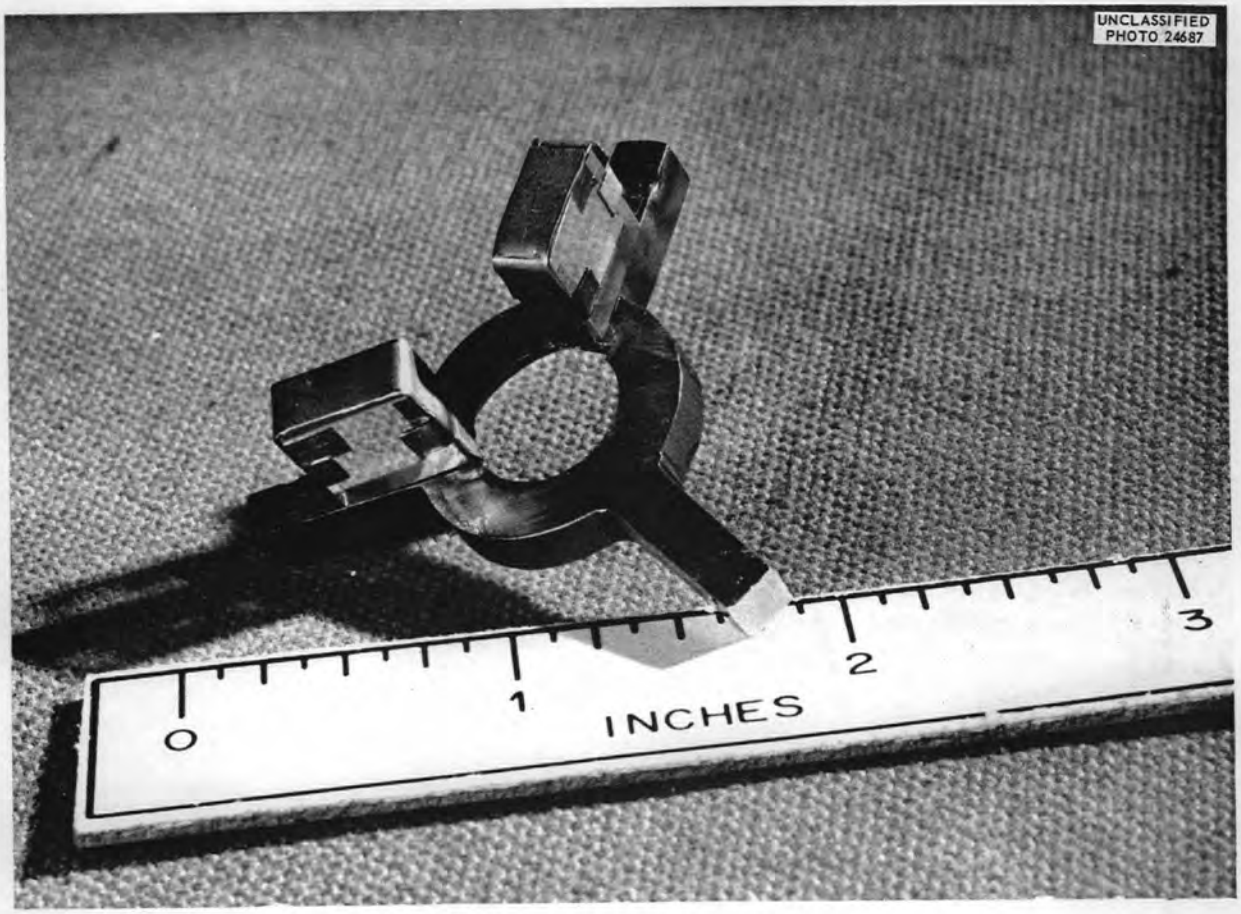

Fig. 7. Core Sapphire Specimens Before Irradiation.

Table 6. Loop Areas Exposed to High Temperature Solution (Type 347 Stainless Steel)

Component	Area Exposed (cm^2)
Total main circulation lines (not including pump and core)	1553
Pressurizer	
Total	(706)
Area wetted when filled with 175 ml of solution	335
Pressurizer lines	300
Core	445
Pump	
Scroll	272
Impeller	159
Total	3064

Exceptionally low flow of solution through the loop pressurizer was noted during almost the entire in-pile operation. As shown in Fig. 8, the pressurizer flow during the first 100 hr of circulation time with enriched solution dropped rapidly from an initial value of 5.1 cc/sec to about 1.2 cc/sec. At this point the reactor was shut down. A variable frequency motor generator set was installed from which the circulating pump was operated for the balance of the experiment at 86 cps instead of at the normal 60 cps line current. This of course gave a corresponding increase in pump speed. The flow rate through the pressurizer immediately increased to 1.5 cc/sec.

It is assumed that the immediate increase in pressurizer flow rate resulted from increased flow through the main stream. Since the two should be proportional, the mainstream flow rate must have increased from the initial 7.3 gpm to about 9.3 gpm. This means that the velocity of solution in the

Table 7. Total Areas Exposed to High Temperature Solution: Stainless Steel Specimens

Component	SS-347		SS-443[a]		SS-446[b]		SS-350A[c]		Total Area (cm^2)
	Number	Total Area (cm^2)	Number	Total Area (cm^2)	Number	Total Area (cm^2)	Number	Total Area (cm^2)	
Core coupons	1	2.1	1	2.1					
In-line coupons	1	2.1	1	2.1					
Core rod coupons	3	11.5	3	11.5	2	7.7	2	7.7	
Special in-line rod coupons	5	19.2	1	3.8	1	3.8	1	3.8	
Core rod assembly spacers	88	293							
Special in-line rod assembly spacers	42	154.2							
Core spiders	2	77							
Sapphire holders	2	6							
Sapphire holder spiders	1	16							
Core rod assembly rods	8	182							
Special in-line rod assembly rods	4	91							
Total		854.1		19.5		11.5		11.5	896.6

[a]Lot #2 hot rolled and annealed.
[b]Lot #2 rolled and pickled.
[c]Item #381 as annealed.

Table 8. Total Areas Exposed to High Temperature Solution: Titanium

Material	Component								Total Area (cm^2)
	Core Coupons		In-Line Coupons		Core Rod Coupons		Special In-Line Rod Coupons		
	Number	Total Area (cm^2)	Number	Total Area (cm^2)	Number	Total Area (cm^2)	Number	Total Area (cm^2)	
Ti-75A, Item #45					2	7.7	6	23	30.7
Ti-110AT, Item #1176	1	2.1	1	2.1	3	11.5	1	3.8	19.5
Ti-130AM, Item #1175	1	2.1	1	2.1	3	11.5	1	3.8	19.5
								Total	69.7

Table 9. Total Areas Exposed to High Temperature Solution: Zirconium and Zirconium Alloys

Material	Component														Total Area (cm^2)
	Core Coupons		In-Line Coupons		Core Rod Coupons		Special In-Line Rod Coupons		Coupon Holders		Core Pin Specimens		Special In-Line Pin Specimens		
	No.	Total Area (cm^2)	No.	Total Area (cm^2)	No.	Total Area (cm^2)	No.	Total Area (cm^2)	No.	Total Area (cm^2)	No.	Total Area (cm^2)	No.	Total Area (cm^2)	
Zircaloy-2															
Item #1157									2	346					346
Cut from Newport News bottom weld	1	2.1	1	2.1											4.2
Cut from Newport News weld					3	11.5									11.5
5 ppm H_2	1	2.1	1	2.1	3	11.5	1	3.8							19.5
1000 ppm H_2	1	2.1	1	2.1	3	11.5	1	3.8							19.5
3000 ppm H_2					2	7.6	1	3.8							11.4
Total Zircaloy-2															412.1
Zircaloy-3															
0.7% Fe											1	5.7	1	5.7	11.4
1.4% Fe											1	5.7	1	5.7	11.4
3.5% Fe											1	5.7	1	5.7	11.4
3.0% Ag	1	2.1	1	2.1	3	11.5	1	3.8							19.5
0.26% Sn, 0.19% Fe, 40 ppm N_2	1	2.1	1	2.1	3	11.5	1	3.8							19.5
0.50% Sn, 0.44% Fe	1	2.1	1	2.1	3	11.5	1	3.8							19.5
0.50% Sn, 0.24% Fe, 0.25% Ni	1	2.1	1	2.1	3	11.5	1	3.8							19.5
1.46% Sn, 0.25% Fe, 0.21% Mo, 50 ppm N_2	1	2.1	1	2.1	3	11.5	1	3.8							19.5
0.47% Sn, 0.85% Fe, 0.78% Ni, 50 ppm N_2	1	2.1	1	2.1	3	11.5	1	3.8							19.5
0.56% Sn, 0.71% W, 60 ppm N_2	1	2.1	1	2.1	3	11.5	1	3.8							19.5
0.52% Sn, 5.71% Ti, 40 ppm N_2	1	2.1	1	2.1	3	11.5	1	3.8							19.5
0.52% Sn, 0.28% Fe, 5.66% Ti, 60 ppm N_2	1	2.1	1	2.1	3	11.5	1	3.8							19.5
0.24% Fe, 0.32% Nb, 70 ppm N_2	1	2.1	1	2.1	3	11.5	1	3.8							19.5
1.54% Sn, 0.26% Fe, 0.83% Nb, 80 ppm N_2	1	2.1	1	2.1	3	11.5	1	3.8							19.5
3.84% Al, 2.5% Mn	1	2.1	1	2.1	3	11.5	1	3.8							19.5
0.69% Sn, 0.69% Cu, 40 ppm N_2	1	2.1	1	2.1	3	11.5	1	3.8							19.5
0.81% Fe, 0.77% Cr					2	7.6	1	3.8							11.4
0.72% Fe, 0.73% Cr, 0.45% Sn					2	7.6	1	3.8							11.4
1.5% Cr, 0.50% Sn					2	7.6	1	3.8							11.4
15% Nb, 500°C 2 hr *in vacuo*, slow cool					2	7.6	1	3.8							11.4
2% Nb					2	7.6	1	3.8							11.4
Total Zircaloy-3															344.7
Zircaloy-4															
0.7% Fe, 2.8 Cr											1	5.7	1	5.7	11.4
Crystal-bar zirconium	1	2.1	1	2.1	3	11.5	1	3.8							19.5
Total zirconium															787.7

Table 10. Total Areas Exposed to High Temperature Solution: Miscellaneous Specimens

Material	Component										Total Area (cm^2)
	Core Coupons		In-Line Coupons		Core Rod Coupons		Special In-Line Rad Coupons		Special Core Sapphire Specimens		
	Number	Total Area (cm^2)	Number	Total Area (cm^2)	Number	Total Area (cm^2)	Number	Total Area (cm^2)	Number	Total Area (cm^2)	
Sapphire									2	9.2	9.2
Sintered aluminum oxide	1	2.1	1	2.1	1	3.8					8.0
Platinum	1	2.1	1	2.1	3	11.5	1	3.8			19.5
Incoloy, Item #275	1	2.1	1	2.1	3	11.5	1	3.8			19.5
										Total	56.2

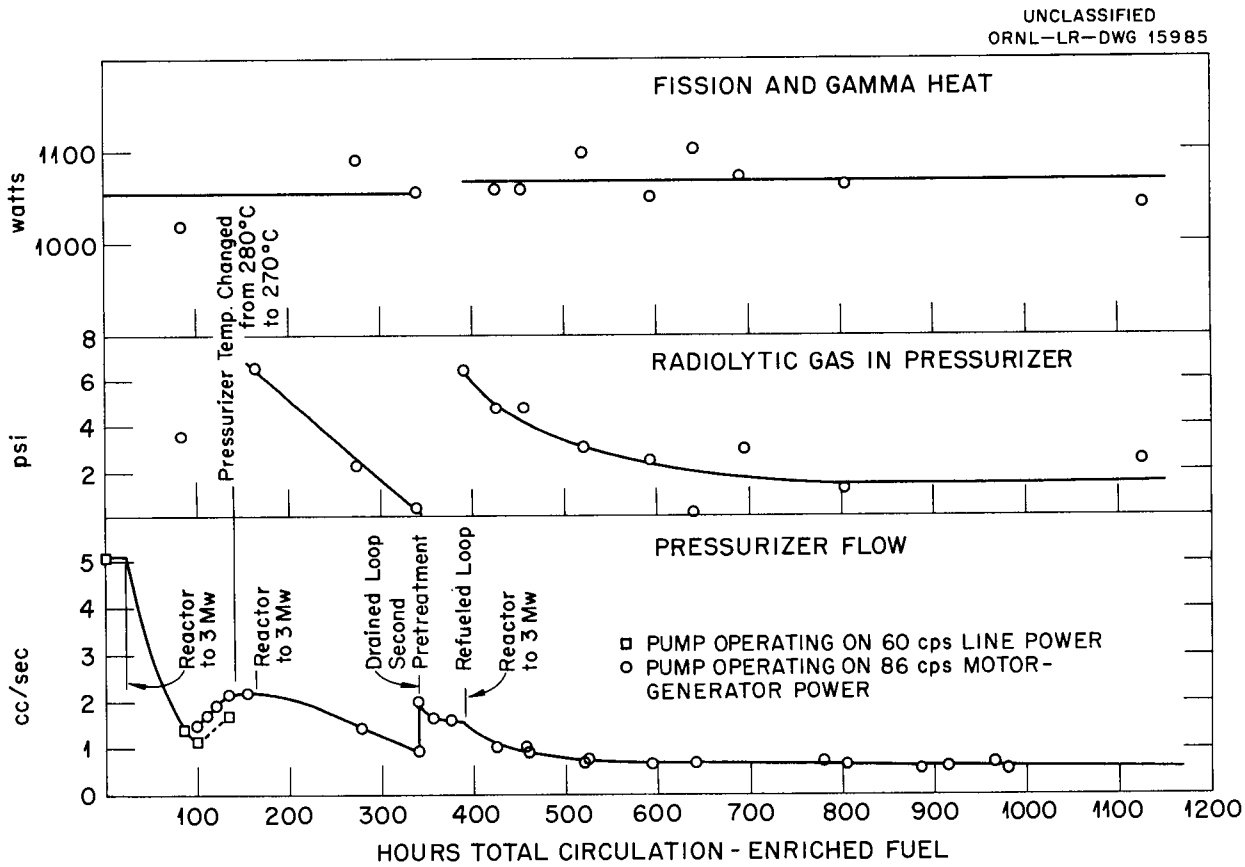

Fig. 8. Fission and Gamma Heat, Radiolytic Gas in Pressurizer, and Pressurizer Flow.

Table 11. Analyses of Samples from Loop Inventory During Preparatory Operations*

Solution	Total Circulation Time for Each Solution (hr)	Inventory at Time of Sampling (ml)	Uranium		Sulfate		Copper		Nickel		Iron		Chromium		Aluminum		Chlorine		pH	Phosphate	
			Conc (mg/ml)	Total (g)	Conc (mg/ml)	Total (g)	Conc (μg/ml)	Total (mg)	Conc (μg/ml)	Total (mg)	Conc (μg/ml)	Total (mg)	Conc (μg/ml)	Total (mg)	Conc (μg/ml)	Total (mg)	Conc (μg/ml)	Total (mg)		Conc (μg/ml)	Total (mg)
First pretreatment																					
3% TSP (He, 100°C)	4	1100					<1	1.0	<1	1.1	1	1.1			1	1.1	<2	2.2	11.35		
5% HNO_3 (He, 100°C)	11	1100					8	8.8	13	14.0	112	123	13	14	10	11	<2	2.2	2.12		
H_2O (O_2, 250°C)	30	1100					<1	1.0	1	1.1	<1	1.1	1	1.1	1	1.1	<1	1.1	4.42		
0.17 M UO_2SO_4 (natural) 0.03 M $CuSO_4$ 0.04 M H_2SO_4	73	1100	34.4	37.8	19.50	21.5	1780	1.65	116	128	10	11	31	34			4	4.4	1.65		
Second pretreatment (after 343.5 hr circulation with enriched solution)																					
H_2O	6	1100																			
3% TSP	6	1300	0.095	0.12					0.0	0.0									11.6		
5% HNO_3	8.5	1300	0.238	0.31					17.0	22.1									0.85		
5% HNO_3	4.7	1300	0.10	0.13					25.0	32.5					0.0	0.0			0.6	0.0	0.0
H_2O	7.7	1100																	6.5		

*Constituent concentrations ond totals shown are not cumulative but represent the quantities present for operation with each solution.

straight channel coupon holders increased from 13.3 fps to about 17 fps for the remainder of the run.

While the reactor was down, an attempt was made to unplug what was assumed to be a partially plugged pressurizer inlet or outlet line by reducing the pressurizer solution temperature to 250°C and raising the loop temperature to 255°C. There was hope that the plug would dissolve or loosen at the lower pressurizer temperature. After 1½ hr at these conditions the pressurizer temperature was raised to 270°C and the loop temperature lowered to 250°C, where they were maintained for the remainder of the run. After the pressurizer flow had gradually risen to 2.2 cc/sec, the reactor was taken to power. During the next 205 hr of operation at power the pressurizer flow decreased to 0.9 cc/sec. At this time the reactor and the loop were shut down and the solution was drained. The accumulated total circulation time for the first original solution was 344 hr. The loop was then given a standard pretreatment operation, as shown in Table 11, and the loop was recharged with fresh solution and operation was resumed. After 45 hr of operation, during which time the pressurizer flow was 2 cc/sec, the reactor was taken to power. During the remaining hours of operation the pressurizer flow decreased to 0.6 cc/sec. After 786 hr of total circulation time with the second original solution, the experiment was terminated.

During the normal shutdown operation the drain line on the loop plugged while the third rinse was being made, and the loop had to be drained through the pump drain line. Since the loop cannot be completely drained through this line, a portion of the rinse water was still in the loop when it was removed from the reactor.

The two original enriched solutions charged to the loop for in-pile operation and the solution used to replace liquid drawn from the loop during sampling operations were of approximately the same composition, as shown in Table 12.

The total circulation time with enriched solution was 1130 hr. The energy output of the LITR during this time was 2175 Mwhr, and essentially all the power was liberated at the 3-Mw level. The reactor operating schedule for the exposure is shown in Fig. 9.

Oxygen partial-pressure measurements were made hourly during the run. When the oxygen partial pressure in the pressurizer was near 40 psi, the reactor was shut down and additional oxygen was added to bring the pressure to about 130 psi.

Two-milliliter samples of solution were taken periodically with the loop at temperature. About 0.2 ml of each sample was used for Cs^{137} analysis. The sampling system was purged with loop solution before a sample was taken; the total volume removed from the circulating stream during the sampling operation was about 8 ml for each sample. The schedule of solution sampling is shown in Table 13. All but eight of the samples taken after loop insertion were withdrawn with the reactor at power. The eight exceptions are shown in Fig. 9 and are summarized in Table 14.

Radiolytic gas pressure measurements were made, usually once per week, by measuring the difference in pressure during reactor operation prior to a shutdown and 30 min after the shutdown. Fission and gamma heat measurements were made at the same time by observing the difference between electric power requirements of the loop heaters during operation at full reactor power and during reactor shutdown.

Table 12. Composition of Enriched Solutions

	Total U (mg/ml)	Calculated Assay (U^{235}/total U)	Copper (mg/ml)	pH	Nickel (mg/ml)
First original solution	38.44	89.71	1.864	1.25	0.504
Second original solution	39.24	92.66	2.140	1.30	0.0
Makeup solution	38.26	88.78	1.939	1.30	0.0

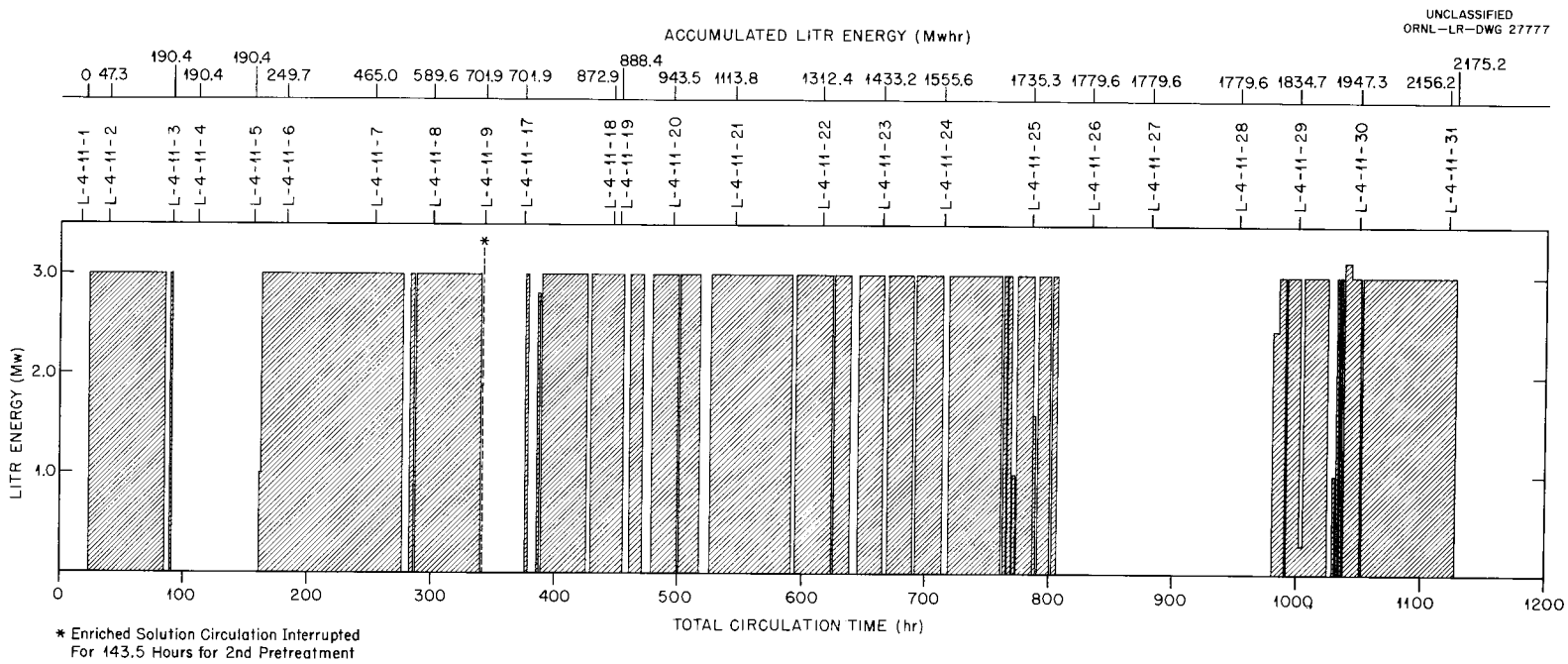

Fig. 9. LITR Operating and Sampling Schedule.

Table 13. Analyses of Samples from Loop Inventory During Enriched-Solution Operation[a]

Sample	Total Circulation Time (hr)	Accumulated LITR Energy (Mwhr)	Inventory Volume at Time of Sample, 25°C (ml)	Lithium[b] (mg/ml)	Sample Dilution Factor[c]	Uranium			Sulfate			Copper			Chromium		Nickel		Chlorine		Iron		Zirconium		Aluminum		Manganese		pH	Specific Gravity
						Rep (mg/ml)	Cor[d] (mg/ml)	Calcd[e] (mg/ml)	Rep (mg/ml)	Cor[f] (mg/ml)	Calcd[e] (mg/ml)	Rep (mg/ml)	Cor[d] (mg/ml)	Calcd[e] (mg/ml)	Cor[d] (mg/ml)	Calcd Total[g] (g)	Cor[d] (mg/ml)	Calcd Total[h] (g)	Cor[d] (mg/ml)	Calcd Total[i] (g)	Cor[d] (mg/ml)	Calcd Total[g] (g)	Cor[d] (mg/ml)	Calcd Total[g] (g)	Cor[d] (mg/ml)	Calcd Total[i] (g)	Cor[d] (mg/ml)	Calcd Total[i] (g)		
First original charge L-4-11-orig	0	0	1102	0	0	38.4	38.4	38.4	24.4	24.4	24.4	1.86	1.86	1.86	(ND)	(ND)	0.504	0.555	(ND)	(ND)	0.001	0.001	(ND)	(ND)	(ND)	(ND)	(ND)	(ND)	1.25	1.063
Make-up solution L-4-8-20	0	0		0	0	38.3	38.3	38.3	24.6	24.6	24.6	1.94	1.94	1.94	(ND)	(ND)	(ND)	(ND)	(ND)	(ND)	(ND)	(ND)	(ND)	(ND)	(ND)	(ND)	(ND)	(ND)	1.30	1.061
L-4-11-1[j]	17.2	0	1093	0.136	1.17	34.5	40.3	38.4	20.4	22.7	24.3	1.95	2.28	1.86	0.032	0.034	0.531	0.035	(ND)	(ND)	0.016	0.018	0.021	0.023	(ND)	(ND)	(ND)	(ND)	1.45	
L-4-11-2	39.8	47.3	1093	0.190	1.25	31.5	39.3	38.4	20.1	23.5	24.3	1.65	2.06	1.86	0.040	0.044	0.543	0.051	(ND)	(ND)	0.015	0.016	0.029	0.032	(ND)	(ND)	(ND)	(ND)	1.50	
L-4-11-3[j]	91.4	190.4	1093	0.163	1.21	32.0	38.6	38.3	21.6	24.7	24.3	1.45	1.74	1.86	0.024	0.026	0.891	0.437	(ND)	(ND)	0.005	0.006	0.025	0.027	(ND)	(ND)	(ND)	(ND)	1.55	
L-4-11-4[j]	111.5	190.4	1091	0.166	1.21	31.9	38.6	38.3	20.4	23.3	24.3	1.39	1.69	1.86	0.064	0.070	1.052	0.625	(ND)	(ND)	0.005	0.006	(ND)	(ND)	(ND)	(ND)	0.124	0.135	1.65	
L-4-11-5[j]	156.5	190.4	1108	0.153	1.19	32.2	38.3	38.3	21.8	24.8	24.3	2.15	2.56	1.86	0.071	0.079	1.206	0.828	(ND)	(ND)	0.043	0.048	0.049	0.054	(ND)	(ND)	0.043	0.050	1.70	
L-4-11-6	182.2	249.7	1100	0.165	1.21	31.1	37.7	38.3	21.6	24.8	24.3	1.49	1.80	1.86	0.211	0.232	1.053	0.670	(ND)	(ND)	0.110	0.121	0.017	0.019	(ND)	(ND)	0.100	0.113	1.55	
L-4-11-7	254.0	465.0	1097	0.170	1.22	32.4	39.4	38.3	21.3	24.5	24.3	1.64	2.00	1.86	0.079	0.087	1.388	1.052	(ND)	(ND)	0.044	0.048	0.017	0.019	(ND)	(ND)	0.122	0.139	1.55	
L-4-11-8	301.6	589.6	1100	0.139	1.17	30.9	36.2	38.3	20.8	23.2	24.2	1.59	1.86	1.86	0.119	0.131	1.614	1.325	(ND)	(ND)	0.045	0.049	0.011	0.012	(ND)	(ND)	0.130	0.150	1.55	
L-4-11-9[j]	342.4	701.9	1098	0.230	1.32	32.3	42.6	38.3	21.0	25.6	24.2	1.21	1.60	1.86	0.071	0.078	1.344	1.056	(ND)	(ND)	0.036	0.039	0.042	0.046	(ND)	(ND)	0.150	0.175	1.80	
Second original charge L-4-11-second orig	0.0	0.0	1116	0.0	0.0	39.2	39.2	39.2	25.7	25.7	25.7	2.14	2.14	2.14	0.012	0.013	(ND)	(ND)	(ND)	(ND)	0.012	0.013	(ND)	(ND)	(ND)	(ND)	(ND)	(ND)	1.30	1.054
Make-up solution L-4-8-20	0.0	0.0		0.0	0.0	38.3	38.3	38.3	24.6	24.6	24.6	1.94	1.94	1.94	(ND)	(ND)	(ND)	(ND)	(ND)	(ND)	(ND)	((ND)	(ND)	(ND)	(ND)	(ND)	(ND)	(ND)	1.30	1.061
L-4-11-17[j]	375.4	701.9	1107	0.141	1.17	33.1	38.9	39.2	22.2	24.9	25.6	1.48	1.74	2.14	0.021	0.023	0.072	0.080	(ND)	(ND)	0.047	0.052	0.063	0.070	0.012	0.013	0.073	0.081	1.40	
L-4-11-18	447.4	872.9	1107	0.163	1.21	33.0	39.9	39.1	23.9	27.5	25.6	1.47	1.77	2.13	0.048	0.053	0.512	0.568	(ND)	(ND)	0.076	0.084	0.052	0.058	0.007	0.008	0.078	0.086	1.55	
L-4-11-24[j]	452.5	888.4	1107					39.1			25.6			2.13																
L-4-11-25	495.3	993.5	1107	0.175	1.23	31.5	38.6	39.1	22.2	25.7	25.6	1.73	2.11	2.13	0.061	0.068	0.555	0.627	(ND)	(ND)	0.061	0.068	(ND)	(ND)	(ND)	(ND)	0.116	0.108	1.55	
L-4-11-26[j]	545.6	1113.8	1108	0.193	1.25	32.7	41.1	39.1	22.4	26.4	25.5	1.56	1.96	2.12	0.128	0.142	0.814	0.926	(ND)	(ND)	0.029	0.032	0.023	0.026	0.011	0.013	0.154	0.176	1.65	
L-4-11-27[j]	615.8	1312.4	1107	0.201	1.27	35.0	44.4	39.0	21.5	25.5	25.5	1.56	1.98	2.12	0.156	0.173	0.884	1.018	(ND)	(ND)	0.038	0.042	0.072	0.080	0.011	0.013	0.132	0.154	1.70	
L-4-11-28[j]	664.6	1433.2	1108	0.204	1.27	31.3	39.9	39.0	21.8	25.9	25.5	1.37	1.74	2.12	0.437	0.484	0.961	1.122	(ND)	(ND)	0.047	0.052	0.053	0.059	(ND)	(ND)	0.136	0.161	1.70	
L-4-11-24[i]	713.5	1555.6	1107	0.197	1.26	31.9	40.3	39.0	22.0	26.0	25.5	1.40	1.77	2.12	0.140	0.155	0.832	1.108	(ND)	(ND)	0.033	0.037	0.016	0.018	0.011	0.013	0.145	0.174	1.70	
L-4-11-25	785.4	1735.3	1107	0.191	1.25	32.1	40.2	39.0	21.5	25.3	25.4	1.49	1.87	2.11	0.184	0.204	1.059	1.266	(ND)	(ND)	0.028	0.031	0.038	0.042	0.009	0.013	0.146	0.178	1.80	
L-4-11-26[i]	833.6	1779.6	1108	0.165	1.21	34.5	41.7	38.9	20.6	23.5	25.4	1.68	2.03	2.11	0.107	0.119	0.948	1.165	(ND)	(ND)	0.023	0.025	0.006	0.007	(ND)	(ND)	0.152	0.188	1.80	
L-4-11-27[i]	881.5	1779.6	1107	0.206	1.28	30.9	39.4	38.9	20.2	23.9	25.4	1.50	1.91	2.11	0.089	0.099	1.236	1.501	(ND)	(ND)	0.041	0.045	(ND)	(ND)	(ND)	(ND)	0.161	0.200	1.80	
L-4-11-28[i]	953.2	1779.6	1108	0.196	1.26	32.2	40.6	38.9	23.7	28.2	25.4	1.43	1.80	2.11	0.166	0.184	1.109	1.386	(ND)	(ND)	0.034	0.038	(ND)	(ND)	(ND)	(ND)	0.136	0.176	1.75	
L-4-11-29	1001.5	1834.7	1108	0.205	1.28	37.4	47.7	38.9	21.9	26.2	25.4	1.85	2.36	2.10	0.092	0.102	1.377	1.705	(ND)	(ND)	0.041	0.045	(ND)	(ND)	(ND)	(ND)	0.185	0.233	1.70	
L-4-11-30	1049.3	1947.3	1106	0.214	1.29	30.1	38.9	38.9	20.8	24.9	25.4	1.35	1.74	2.10	0.052	0.058	1.202	1.536	(ND)	(ND)	0.015	0.017	(ND)	(ND)	(ND)	(ND)	0.167	0.217	1.85	
L-4-11-31	1121.4	2156.2	1107	0.209	1.26	30.7	38.9	38.9	21.4	25.6	25.4	1.37	1.76	2.10	0.022	0.024	1.510	1.900	(ND)	(ND)	0.035	0.039	(ND)	(ND)	(ND)	(ND)	0.208	0.265	1.80	
Reactor down	1127.8	2175.2	1107																											

[a]Where no values are given, either an analysis was not requested or the analytical results were not reliable. ND, not detected.
[b]Wash water contained Li_2SO_4 at 0.0684 M.
[c]Dilution factors calculated on lithium concentration found in sample.
[d](Reported concentration) × (dilution factor).
[e]Determined from calculated uranium, copper, or sulfate inventory balances.
[f](Reported concentration) × (dilution factor); corrected for sulfate from Li_2SO_4.
[g](Reported concentration) × (dilution factor) × (inventory volume).
[h](Reported concentration corrected for sample dilution, amounts withdrawn in previous samples, and less amount present from original solution) × (inventory volume).
[i](Reported concentration corrected for sample dilution and amounts withdrawn in previous samples) × (inventory volume).
[j]Sample taken with reactor down.

Table 14. Samples Taken with Reactor Down

Sample No.	Reactor Down (hr)
L-4-11-3	0.8
L-4-11-4	20.9
L-4-11-5	65.9
L-4-11-9	2.4
L-4-11-24	0.4
L-4-11-26	27.8
L-4-11-27	75.9
L-4-11-28	147.4

Pressurizer flow measurements were made by observing the difference in the electric power requirements for the pressurizer heater at two different loop temperatures.

Dismantling

The loop was dismantled without any significant difficulties. The core and two in-line sample holders were transferred to the corrosion examination facility for disassembly and inspection. Four sections of the main line piping were transferred to the Chemical Technology Division for decontamination studies. The pressurizer and the attached inlet and outlet lines were removed as a unit, and flow measurements were made through this system in an effort to locate the cause of the reduced pressurizer flow encountered during operation. This component was then disassembled and examined in the corrosion examination facility. The pump was separated from the remainder of the loop, and the flange bolts and volute seal weld were cut in the dismantling cell. Portions of the loop not retained for further evaluation were sent to the burial ground and stored in hole No. 193.

Representative samples of Incoloy and zirconium alloys were taken from the core holder and core rod assemblies, decontaminated, and sent to the Analytical Chemistry Division for induced activity determinations. These specimens were compared with irradiated control specimens which had been exposed along with standard cobalt samples in the LITR.

Various sections of the steel loop components together with several of the titanium and zirconium alloy specimens were sent to the Solid State Division for metallographic examination.

RESULTS

Oxygen-Consumption Data

The results of oxygen-consumption measurements are shown in Table 15. The values for corrosion penetration listed in the final column of Table 15 were calculated with the assumption that all steel surfaces in contact with high temperature solution corroded uniformly and that oxygen was consumed in the corrosion of steel only. The average quantity of oxygen in the loop at a given oxygen partial pressure was 13.4 cc(STP)/psi at 280°C and 12.4 cc(STP)/psi at 270°C. As calculated from the oxygen data, the corrosion rate for the first 110 hr of operation was 5.0 mpy. For the next 232 hr the rate was 1.7 mpy. With the second fuel solution, the corrosion rate was 7.2 mpy for the first 120 hr of operation and 1.9 mpy for the remaining 666 hr of the run. A plot of oxygen consumption against circulation time is shown in Fig. 10.

Solution Analyses

The results of solution analyses for constituents other than fission products are tabulated in Table 13. Sample L-4-11-9 was taken just before the first enriched solution was drained from the loop. Similarly, sample L-4-11-31 was taken just before the second enriched solution was drained from the loop.

Calculated values for the total amounts of corrosion products for the entire in-pile run are the sums of the values for L-4-11-9 and L-4-11-31. Since the first enriched solution charged to the loop contained added nickel, the calculated value of nickel in the solution at the time of taking samples L-4-11-1 through L-4-11-9 has been corrected for the amount of the initial added nickel remaining in the inventory at the time of sampling. The calculated values for the total amounts of corrosion products for all samples have been corrected for sample dilution and for the amounts previously withdrawn in sampling.

As was observed during all previous experiments, the reported values for the uranium, copper, and sulfate content of the samples from this loop were found to be, in general, appreciably lower than the calculated values for these constituents. Applying dilution factors based on the amount of lithium tracer found in the samples, the corrected concentrations were in most cases in better

Table 15. Oxygen Consumption in Loop

Remarks	Sample No.	LITR Energy (Mwhr)	Total Solution Circulation Time (hr)	O_2 Additions to Loop (cc at STP)	O_2 Withdrawn from Loop* (cc at STP)	Total O_2 Charged to Loop Less O_2 Withdrawn in Sampling (cc at STP)	O_2 Volume at Time of Sample (cc at STP)	O_2 Consumed Since Last Sample (cc at STP)	Total O_2 Consumed (cc at STP)	Calculated Corrosion Penetration of Type 347 Stainless Steel (mils)
				Operation with 1st Enriched Solution						
O_2 addition (L-4-11-3)		0	0	1487	0	1487	1487	0	0	0
	L-4-11-1**	0	17.2	0	0	1487	1487	0	0	0
	L-4-11-2	47.3	39.8	0	10	1477	1339	138	138	0.006
O_2 addition (L-4-11-4)				881	9	2349				
	L-4-11-3**	190.4	91.4	0	0	2349	1274	937	1075	0.05
	L-4-11-4**	190.4	111.5	0	8	2341	846	420	1495	0.06
O_2 addition (L-4-11-5)				1199	5	3535				
	L-4-11-5**	190.4	156.5	0	0	3535	1920	120	1615	0.07
	L-4-11-6	249.7	182.2	0	8	3527	1685	227	1842	0.08
	L-4-11-7	465.0	254.0	0	8	3519	1345	332	2174	0.09
O_2 addition (L-4-11-6)				576	6	4089				
	L-4-11-8	589.6	301.6	0	0	4089	1675	240	2414	0.10
	L-4-11-9**	701.9	342.4	0	8	4081	1511	156	2570	0.11
Pump off		701.9	345.5	0	0	4081				
Solution drained		701.9	345.5	0	1511	2570				
				Operation with 2nd Enriched Solution						
O_2 addition (L-4-11-7)		701.9		1624	0	4194	1533		2661	
	L-4-11-17**	701.9	377.4	0	0	4194	1533	91	2661	0.11

*Calculated amount removed as O_2 dissolved in sample.

**Samples taken with reactor down.

Table 15 (continued)

Remarks	Sample No.	LITR Energy (Mwhr)	Total Solution Circulation Time (hr)	O_2 Additions to Loop (cc at STP)	O_2 Withdrawn from Loop* (cc at STP)	Total O_2 Charged to Loop Less O_2 Withdrawn in Sampling (cc at STP)	O_2 Volume at Time of Sample (cc at STP)	O_2 Consumed Since Last Sample (cc at STP)	Total O_2 Consumed (cc at STP)	Calculated Corrosion Penetration of Type 347 Stainless Steel (mils)
				Operation with 2nd Enriched Solution						
O_2 addition (L-4-11-8)				843	9	5028				
	L-4-11-18	872.9	449.5	0	0	5028	890	1477	4138	0.18
	L-4-11-19	888.4	454	0	6	5022	778	106	4244	0.18
O_2 addition (L-4-11-9)				774	5	5791				
	L-4-11-20	993.5	497.3	0	0	5791	799	748	4992	0.21
O_2 addition (L-4-11-10)				712	5	6498				
	L-4-11-21	1113.8	547.7	0	0	6498	1228	278	5270	0.22
	L-4-11-22	1312.4	617.8	0	7	6491	895	326	5596	0.24
O_2 addition (L-4-11-11)				626	5	7112				
	L-4-11-23	1433.2	665.5	0	0	7112	1208	308	5904	0.25
	L-4-11-24**	1555.6	713.5	0	8	7104	1001	199	6103	0.26
	L-4-11-25	1735.3	785.4	0	7	7097	731	263	6366	0.27
O_2 addition (L-4-11-12)				766	5	7858				
	L-4-11-26**	1779.6	833.6	0	0	7858	1385	107	6473	0.28
	L-4-11-27**	1779.6	881.5	0	8	7850	1036	341	6814	0.29
	L-4-11-28**	1779.6	953.2	0	6	7844	512	518	7332	0.31
O_2 addition (L-4-11-13)				1016	3	8857				
	L-4-11-29	1834.7	1001.5	0	0	8857	1262	263	7595	0.32
	L-4-11-30	1947.3	1049.3	0	8	8849	1032	222	7817	0.33
	L-4-11-31	2156.2	1121.4	0	6	8843	682	344	8161	0.35
End of Run		2156.2	1130.1	0	4	8839	639	39	8200	0.35

*Calculated amount removed as O_2 dissolved in sample.

**Samples taken with reactor down.

agreement with the calculated concentrations for these constituents. The reported, corrected, and calculated values for the uranium, copper, and sulfate concentrations are compared graphically in Fig. 11. The calculated values for the other elements listed in Table 13 and the corrected values for total fissions in Table 16 have been obtained through use of the listed dilutions. No correction was applied to pH measurements.

The nickel and manganese data given in Table 13 are plotted against circulation time in Fig. 10. Also shown on another ordinate in Fig. 10 is the

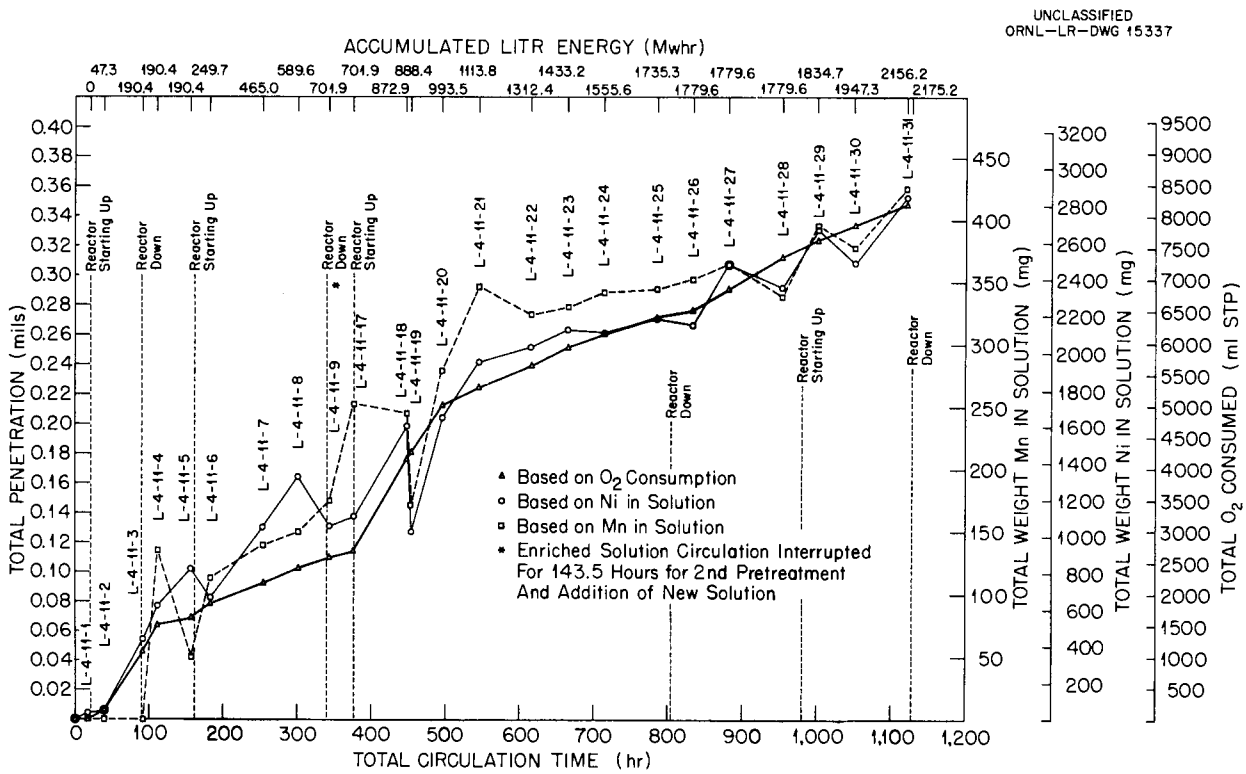

Fig. 10. Over-All Stainless Steel Corrosion Penetration.

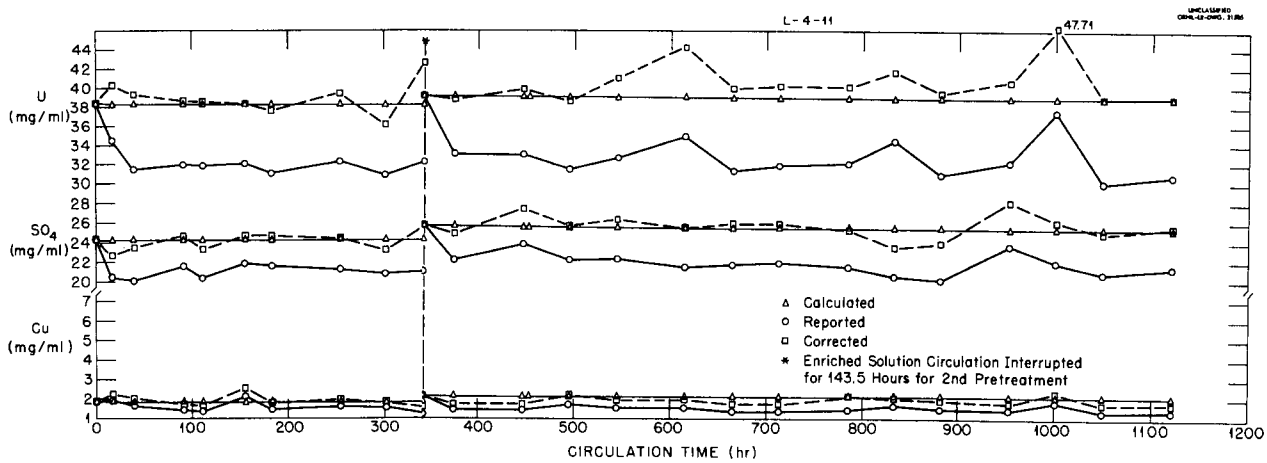

Fig. 11. Comparison of Reported, Corrected, and Calculated Uranium, Sulfate, and Copper Concentrations for Enriched Solution Operations.

Table 16. Fissions in Loop Solution

Sample No.	Accumulated LITR Energy (Mwhr)	Inventory Volume at Time of Sample (ml at 25°C)	Calculated Uranium Concentration (mg/ml)	Total Fissions per Milliliter		Total Fission Power in Loop Solution at 3 Mw (w)
				Analysis	Corrected*	
			Operation with 1st Enriched Solution			
				$\times 10^{15}$	$\times 10^{15}$	
L-4-11-1	0	1093	38.4			
L-4-11-2	47.3	1093	38.4	1.13	1.41	867
L-4-11-3	190.4	1093	38.3	4.05	4.91	750
L-4-11-4	190.4	1091	38.3	3.70	4.55	694
L-4-11-5	190.4	1108	38.3	4.06	4.95	767
L-4-11-6	249.7	1100	38.3	4.50	5.62	659
L-4-11-7	465.0	1097	38.3	8.78	10.9	684
L-4-11-8	589.6	1100	38.3	11.7	14.0	695
L-4-11-9	701.9	1098	38.3	13.1	17.8	741
			Operation with 2nd Enriched Solution			
L-4-11-17	0	1107	39.2			
L-4-11-18	171.0	1107	39.1	3.50	4.22	727
L-4-11-19	186.5	1107	39.1			
L-4-11-20	291.6	1107	39.1	4.87	6.02	608
L-4-11-21	411.9	1108	39.1	7.26	9.22	660
L-4-11-22	610.5	1107	39.0	10.7	13.8	666
L-4-11-23	731.3	1108	39.0	14.0	18.2	734
L-4-11-24	853.7	1107	39.0	17.3	22.4	774
L-4-11-25	1033.4	1107	39.0	18.3	23.7	676
L-4-11-26	1077.7	1108	38.9			
L-4-11-27	1077.7	1107	38.9	19.1	25.4	695
L-4-11-28	1077.7	1108	38.9	19.6	26.0	712
L-4-11-29	1132.8	1108	38.9	19.2	26.1	680
L-4-11-30	1245.4	1106	38.9	22.2	30.6	724
L-4-11-31	1454.3	1107	38.9	24.1	33.1	671
					Av	709

*Corrected to include amounts withdrawn in previous samples and for sample dilution.

corrosion penetration of the type 347 stainless steel, based on the nickel and manganese data. This plot is based on the assumption that all steel surfaces in contact with the high temperature solution corroded uniformly.

Free Acid Concentration

The change in free H_2SO_4 concentration in the loop solution with circulation time has been calculated. The calculations are based on the assumption that the nickel and manganese produced during the corrosion process consume the acid mole for mole and that no production of hydrogen ions takes place during the corrosion process. The amount of nickel and manganese produced and the calculated free acid in solution at the time of each sample are given in Table 17. Figure 12 is a plot of the nickel, manganese, and free acid in solution vs circulation time.

Uranium Balance

The balance sheet for the uranium charged to and recovered from the loop is shown in Table 18. The weigh tank was emptied once during operation and again at the end of operation. Material collected before the first emptying is designated as

Table 17. Calculated Free H_2SO_4 in Solution

Sample No.	Inventory (ml)	Circulation Time (hr)	Nickel* and Manganese* Produced at Time of Sample (moles)	Calculated Free Acid in Solution at Time of Sample (moles)
First original charge	1093	0.0	0.0	0.0437
L-4-11-1	1093	17.2	0.0006	0.0431
L-4-11-2	1093	39.8	0.0009	0.0429
L-4-11-3	1093	91.4	0.0074	0.0362
L-4-11-4	1091	111.5	0.0131	0.0306
L-4-11-5	1108	156.5	0.0149	0.0293
L-4-11-6	1100	182.2	0.0133	0.0308
L-4-11-7	1097	254.0	0.0202	0.0239
L-4-11-8	1100	301.6	0.0239	0.0205
L-4-11-9	1098	342.4	0.0206	0.0239
Second original charge	1107	0.0	0.0	0.0443
L-4-11-17	1107	375.4	0.0028	0.0415
L-4-11-18	1107	447.4	0.0112	0.0330
L-4-11-19	1107	452.5		
L-4-11-20	1107	495.3	0.0126	0.0290
L-4-11-21	1108	545.6	0.0188	0.0230
L-4-11-22	1107	615.8	0.0199	0.0222
L-4-11-23	1108	664.6	0.0217	0.0206
L-4-11-24	1107	713.5	0.0215	0.0210
L-4-11-25	1107	785.4	0.0242	0.0186
L-4-11-26	1108	833.6	0.0225	0.0204
L-4-11-27	1107	881.5	0.0283	0.0148
L-4-11-28	1108	953.2	0.0258	0.0177
L-4-11-29	1108	1001.5	0.0321	0.0117
L-4-11-30	1106	1049.3	0.0288	0.0153
L-4-11-31	1107	1121.4	0.0357	0.0087

*Includes amounts withdrawn in previous samples.

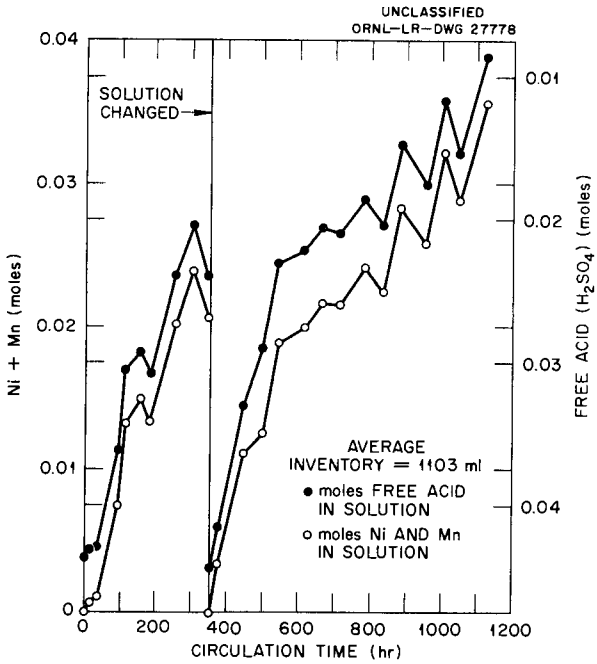

Fig. 12. Nickel plus Manganese and Free Acid in Solution.

first weigh tank; that collected afterward is designated as second weigh tank. Analytical results indicated that 7.9% more uranium was recovered than was originally charged to the loop.

Neutron Flux, Fission Power, and Gamma Heat

The neutron flux at a given specimen position in the core was determined from the induced activity measurements. The Cr^{51} activity was employed for the Incoloy determinations and the Zr^{95}-Nb^{95} activity was employed for the zirconium determinations. The results of these determinations are given in Table 19. In Fig. 13 the logarithms of the neutron fluxes of the specimens are plotted against the position of the specimens. From this plot the neutron flux along the length of the core can be used to calculate the corresponding fission power density. The power densities thus determined ranged from 7.2 w/ml at the leading core-holder coupon to 1.3 w/ml at the rear. The calculations were based on a value of 200 Mev for the average energy per fission.

Table 18. Actual Uranium Balance
Enriched Solution Operation

Source	Solution Weight (g)	Specific Gravity	Solution Volume (ml)	Total Uranium Concentration by Analysis (mg/ml)	Total Uranium (g)
			Charged to Loop		
Original solution charged to loop	1171.2	1.063	1101.8	38.44	42.35
Second solution charged to loop	1176.1	1.054	1115.8	39.24	43.78
Solution additions to loop during operation (fuel expansion)	452.6[a]	1.061	426.6	38.26	16.32
				Total	102.45
			Recovered from Loop		
Loop inventory samples sent to laboratory			55.20		2.21
Weigh tank samples sent to laboratory	13.05[a]	1.0[b]	13.05	5.81–6.48	0.08
First weigh tank contents	8409[c]	1.0[b]	8409	5.956	50.08
Second weigh tank contents	8938[c]	1.0[b]	8938	6.503	58.12
				Total	110.49

[a]Calculated. [b]Assumed. [c]From weigh tank reading.

Table 19. Induced Activity in Specimens

Specimen No.	Cleaned Weight When Counted (g)	Relative Zr^{95}-Nb^{95} Activity 0.76 Mev Gamma (counts·min^{-1}·g^{-1})	Relative Cr^{51} Activity (counts·min^{-1}·g^{-1})	Specimen Exposure Time: Period	Specimen Exposure Time: Total (hr)	Specimen Exposure Time: Equivalent Time at 3 Mw (Mwhr/3 Mw)	Cooling Time Before Analysis (hr)	Neutron Flux at 3 Mw (neutrons·cm^{-2}·sec^{-1})	Power Density at 3 Mw (w/ml)	Distance from Leading Edge of 1st Coupon (in.)
Core Coupons										
								$\times 10^{12}$		
Zircaloy-2 (500 ppm H_2)										
Z-50	0.7577	2.35		1st	62	62	5424	1.374	1.79	4.875
				2nd	645	530	4560			
				3rd	146	132	4248			
Zircaloy-3 (1.46% Sn, 0.25% Fe, 0.21% Mo, 50 ppm N_2)										
ZG-1	0.7494	3.71		1st	62	62	5424	4.26	5.72	2.375
				2nd	645	530	4560			
				3rd	146	132	4248			
Zircaloy-3 (0.52% Sn, 5.71% Ti, 40 ppm N_2)										
ZK-1	0.7335	2.37		1st	62	62	5424	2.09	2.80	3.125
				2nd	645	530	4560			
				3rd	146	132	4248			
Zircaloy-3 (0.26% Sn, 0.19% Fe, 40 ppm N_2)										
ZD-1	0.7643	1.83		1st	62	62	5424	2.81	3.78	1.625
				2nd	645	530	4560			
				3rd	146	132	4248			
Zircaloy-3 (1.54% Sn, 0.26% Fe, 0.83% Nb, 80 ppm N_2)										
ZN-1	0.8061	1.41		1st	62	62	5424	1.70	2.28	3.875
				2nd	645	530	4560			
				3rd	146	132	4248			
Incoloy (Item #275)										
IN-1	0.9702		0.54	1st	62	62	5640	0.97	1.31	2.625
				2nd	645	530	4776			
				3rd	146	132	4464			
Zircaloy-2 (cut from Newport News bottom weld)										
WB-1	0.7438	1.97		1st	62	62	6312	5.93	7.97	0.875
				2nd	645	530	5448			
				3rd	146	132	5136			
Zircaloy-3 (3% Ag)										
ZC-1	0.6219	0.853		1st	62	62	6216	1.39	1.87	4.625
				2nd	645	530	5352			
				3rd	146	132	5040			
Core Rod Coupons										
Zircaloy-2 (500 ppm H_2)										
ZH-11	1.1963	2.77		1st	62	62	5424	1.620	2.11	4.313
				2nd	645	530	4560			
				3rd	146	132	4248			
Zircaloy-3 (1.46% Sn, 0.25% Fe, 0.21% Mo, 50 ppm N_2)										
ZG-18	1.2216	1.59		1st	62	62	5424	1.824	2.45	3.913
				2nd	645	530	4560			
				3rd	146	132	4248			
Zircaloy-3 (0.52% Sn, 5.71% Ti, 40 ppm N_2)										
ZK-11	1.2445	2.74		1st	62	62	5424	2.410	3.24	2.813
				2nd	645	530	4560			
				3rd	146	132	4248			

Table 19 (continued)

Specimen No.	Cleaned Weight When Counted (g)	Relative Zr^{95}-Nb^{95} Activity 0.76 Mev Gamma (counts·min^{-1}·g^{-1})	Relative Cr^{51} Activity (counts·min^{-1}·g^{-1})	Specimen Exposure Time			Cooling Time Before Analysis (hr)	Neutron Flux at 3 Mw (neutrons·cm^{-2}·sec^{-1})	Power Density at 3 Mw (w/ml)	Distance from Leading Edge of 1st Coupon (in.)
				Period	Total (hr)	Equivalent Time at 3 Mw (Mwhr/3 Mw)				
Core Rod Coupons										
								$\times 10^{12}$		
Zircaloy-3 (0.26% Sn, 0.19% Fe, 40 ppm N_2)										
ZD-7	0.9564	2.47		1st	62	62	5424	3.797	5.10	1.313
				2nd	645	530	4560			
				3rd	146	132	4248			
Zircaloy-3 (1.54% Sn, 0.26% Fe, 0.83% Nb, 80 ppm N_2)										
None returned				1st	62	62	5424			
				2nd	645	530	4560			
				3rd	146	132	4248			
Incoloy (Item #275)										
IN-13	1.6480		1.17	1st	62	62	5640	2.107	2.84	3.113
				2nd	645	530	4776			
				3rd	146	132	4464			
Zircaloy-2 (cut from Newport News weld)										
WC-1	1.1288	2.43		1st	62	62	6312	7.313	9.819	1.113
				2nd	645	530	5448			
				3rd	146	132	5136			
Zircaloy-3 (3% Ag)										
ZC-7	1.0014	1.07		1st	62	62	6216	1.747	2.346	4.413
				2nd	645	530	5352			
				3rd	146	132	5040			
Control Specimens										
Zircaloy-2 (500 ppm)										
Z-60	0.7937	1.0			32.0		4848	12.0		
Zircaloy-3 (1.46% Sn, 0.25% Fe, 0.21% Mo, 50 ppm N_2)										
ZG-3	0.8092	1.0			57.92		3984	10.5		
Zircaloy-3 (0.52% Sn, 5.71% Ti, 40 ppm N_2)										
ZK-3	0.7702	1.0			57.92		3984	8.05		
Zircaloy-3 (0.26% Sn, 0.19% Fe, 40 ppm N_2)										
ZD-3	0.7490	1.0			61.0		4080	13.9		
Zircaloy-3 (1.54% Sn, 0.26% Fe, 0.83% Nb, 80 ppm N_2)										
ZN-3	0.7943	1.0			61.7		3912	10.1		
Incoloy (Item #275)										
IN-3	0.9741		1.0		61.0		4248	10.2		
Zircaloy-2										
WB-4	0.7933	1.0			61.83		4632	13.6		
Zircaloy-3 (3% Ag)										
ZC-2	0.7644	1.0			61.7		4704	13.5		

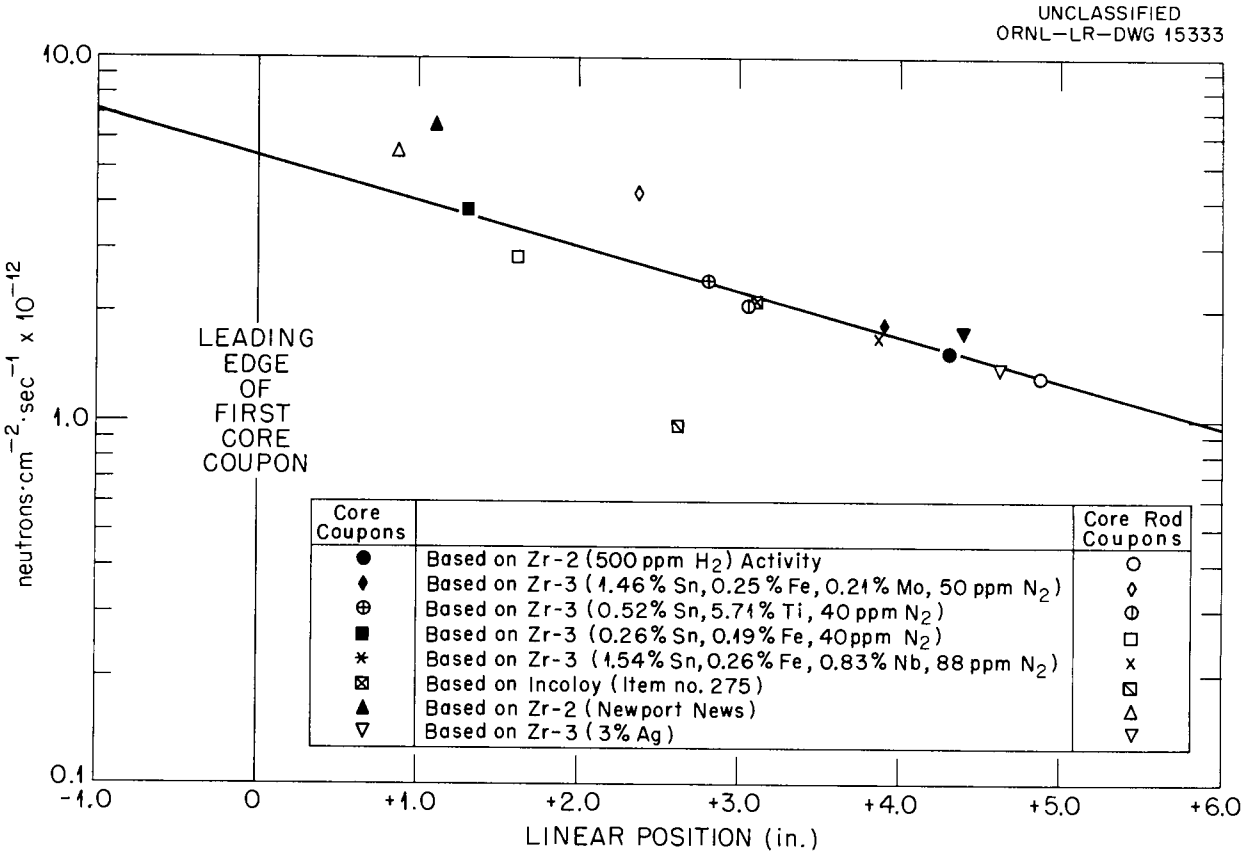

Fig. 13. Flux in Core.

The fission power generated in the loop has been determined by using the Cs^{137} analytical results for calculating total fissions in the experiment. The samples were allowed to decay three months before the final analyses were made. The values calculated are given in Table 9. Each value represents the average power between samples.

The average combined fission and gamma heat, as determined by electrical power differences,[7] was 1054 ± 63 watts during the initial operation and 1067 ± 14 watts after the refueling of the loop. The average combined fission and gamma heat is plotted against the circulation time in Fig. 8.

As in experiments GG (ref 8), EE (ref 9), and L-4-8 (ref 10), there was a fuel element directly in front of hole HB-4 in position C-58 of the LITR lattice during this run. However, the fuel element between holes HB-4 and HB-5 in position C-56 was replaced prior to startup of this experiment with an element containing 68% more U^{235} than the element previously in this location. The value for total fission power, calculated from solution analyses for Cs^{137}, is about 15% higher than in the previous experiment,[10] L-4-8. A corresponding 16% increase in the combined fission and gamma heat was also noted. The volume of solution in the core in both experiments was the same. However, an integrated value for neutron flux in the core, from specimen activity data, is 46% higher in this experiment than in L-4-8. Some major operating variables in previous experiments are given in Table 20.

Radiolytic Gas Pressure

The radiolytic gas pressure in the pressurizer varied with changing flow through the pressurizer. The pressurizer flow rate and the radiolytic gas pressure in the pressurizer are plotted against the circulation time in Fig. 8.

[7] E. J. Walter, *Operation of In-Pile Loop L-4-11*, ORNL CF-56-8-1 (Aug. 1, 1956).

[8] G. H. Jenks *et al.*, *HRP Quar. Prog. Rep. July 31, 1955*, ORNL-1943, p 109–125 (classified).

[9] G. H. Jenks *et al.*, *HRP Quar. Prog. Rep. Oct. 31, 1955*, ORNL-2004, p 121–152 (classified).

[10] J. E. Baker *et al.*, *HRP Radiation Corrosion Studies: In-Pile Loop L-4-8*, ORNL-2042 (Aug. 21, 1956).

Qualitative Inspection of Loop

As with previous loop experiments, all stainless steel surfaces outside the core were covered with a heavy, rust-like scale. The deposit of scale in the pressurizer was found to be heavier in the liquid phase than in the vapor phase region. There was no apparent localized attack on any of the steel components inspected.

Both in-line sample arrays were covered with a bulky, rust-like scale. Figure 14 is a photograph of the in-line coupon array after opening. The sintered alumina coupon in the in-line holder had disintegrated. There was a white oxide film under the bulky, white deposit which completely covered the zirconium alloy containing aluminum and manganese. Otherwise, all in-line holder coupons had the same general appearance. As with all previous loops, cathodic defilming of the in-line coupons was only partially effective, and some film was retained by the coupons. In fact, all but two of the zirconium alloy coupons showed weight

Table 20. Some Major Operating Variables for Loops Containing Zircaloy-2 Core Coupons

Loop	Circulating Time (hr)	LITR Energy (Mwhr)	Per Cent of Operating Time with LITR at Power	Fission and Gamma Heat (w)	Initial Solution[a]				
					U (mg/ml)	Cu (*m*)	H_2SO_4 (*m*)	Cr (ppm)	Ni (ppm)
FF	640	1400	67.6	877	40.0	0.031	0.04		
GG	1060	2700	84.9	1100	40.0	0.031	0.04	320	
EE	630	1610	85.2	837	40.0	0.031	0.008[b]		
L-4-8	1676	4377	87.1	925[c]	40.0	0.031	0.04		
L-4-11	1130	2175	64.2	1065	40.0	0.031	0.04		504

[a]Solution removed from inventory during sampling replaced by solution of similar composition.

[b]Makeup solution contained 0.04 *m* H_2SO_4.

[c]Removal of ANP experiment during operation of this loop caused increase from 825 to 1000 w which decreased to 970 w at termination of the experiment.

UNCLASSIFIED
PHOTO 16479

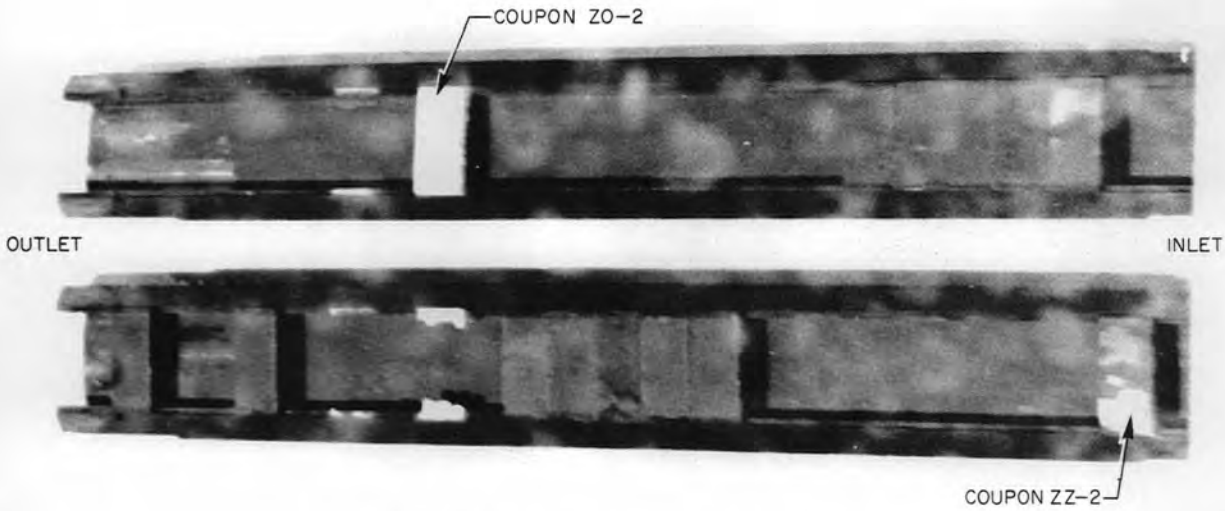

Fig. 14. In-Line Coupon Assembly After Exposure.

gains following the final defilming. Some peculiarities in attack were observed on the defilmed Zircaloy-2 in-line coupon holder. The middle portions of both halves on both inside and outside surfaces were heavily etched, while the ends of the holder retained their smooth machined surfaces.

The core, upon dismantling, was found to be full of solution, probably rinse water, which could not be completely drained from the system upon completion of the experiment. As seen in Fig. 15, all surfaces in the core were found to be coated with a dark, loosely adherent deposit – possibly a result of having remained in contact with the solution for several weeks between the termination of the experiment and the dismantling of the loop. This is the first loop in which any appreciable scale was retained on the Zircaloy-2 core holder coupons. When the core holder was opened, the coupons were dislodged from their original locations, as shown in Fig. 16, but the usual inverse relationship between flux and accumulated film could be seen on the interior surfaces of the coupon holder. Since non-tapered coupon holders had been used, no effect of solution velocity gradients could be observed on the filmed surfaces.

The single sintered alumina coupon in the core holder disintegrated, but a small piece of the single core rod coupon was found intact. This fell apart on handling. Two core rod coupon assemblies, A and H, were very difficult to disassemble. The coupons could not be completely removed from the rod until the rod assemblies had been cathodically defilmed.

The two synthetic sapphire specimens, upon removal from the core, were found to be partially covered with a dark brown film. Places not filmed over were observed to be translucent. Following defilming, the sapphires were an amber color and translucent. A photograph of these specimens taken after irradiation is shown in Fig. 17.

A brief description of each specimen from the loop, as removed and following defilming, is given in Table 21.

This was the second loop in which the pump was outfitted with outboard bearings of sintered aluminum oxide. This pump is the first to perform satisfactorily throughout the entire operation of a loop. However, in view of the loss of the sintered alumina coupons the pump was completely dismantled and inspected. As reported previously,[11] the pump was in excellent condition and there was no measurable wear on any of the alumina bearing surfaces. No localized attack was noted on the pump impeller and volute.

As mentioned above, a flow test was made on the pressurizer circuit after the loop was dismantled. Pressure drops resulting from a water

[11] A. R. Olsen, *Examination of In-Pile Loop Pumps from Loops EE and L-4-11*, ORNL CF-56-6-135 (June 18, 1956).

UNCLASSIFIED
PHOTO 16339

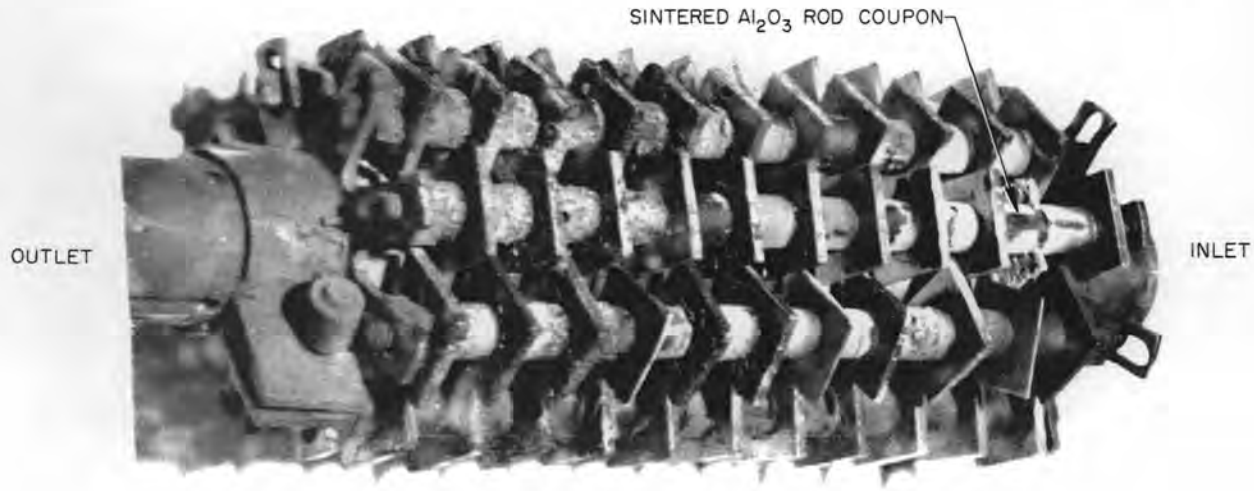

Fig. 15. Core Specimen Assembly After Exposure.

Table 21. Data for Corrosion Specimens

Sample No.	Position	Flow Velocity (fps)	Weight Data: Initial (g)	Weight Data: As Removed (g)	Weight Data: Defilmed (g)	Weight Data: Change (mg)	Exposed Sample Area (cm^2)	Corrosion Penetration (mils)	Corrosion Rate* (Exposed Area) (mpy): 1128 hr	Corrosion Rate* (Exposed Area) (mpy): 725 hr	Total Area (cm^2)	Corrosion Penetration (mils)	Corrosion Rate* (Total Area) (mpy): 1128 hr	Corrosion Rate* (Total Area) (mpy): 725 hr	Distance from Front of First Specimen to Center of Specimen (in.)	Neutron Flux at Specimen Locations (neutrons·cm^{-2}·sec^{-1})	Power Density at Specimen Locations (w/ml)	Appearance: As Removed	Appearance: Defilmed
I. 24 Core Corrosion Sample Coupons																			
A. Platinum																$\times 10^{12}$			
PT-10	1	13 and 17	2.5385	2.5383	2.5383	−0.2	1.57	0.0023	0.018	0.028	2.1	0.0017	0.013	0.020	0.125	5.20	6.98	Light-brown stain over all surfaces	Bright shiny surfaces
B. Alumina																			
Al_2O_3	2	13 and 17	0.4530				1.40				2.1				0.375	4.86	6.53	(Specimen disintegrated)	
C. Crystal-Bar Zirconium																			
ZZ-1	3	13 and 17	0.7951	0.7874	0.7873	−7.8	1.40	0.337	2.61	4.06	2.1	0.225	1.74	2.71	0.625	4.50	6.04	Light-brown stain over all surfaces	No scale; thin gray film with a metallic luster on all surfaces
D. Zircaloy-2																			
WB-1	4	13 and 17	0.7890	0.7818	0.7814	−7.6	1.40	0.329	2.55	3.96	2.1	0.219	1.70	2.64	0.875	4.20	5.64	Light-brown stain over all surfaces	No scale; thin gray film with a metallic luster on all surfaces; brown stain on one side
Z-50	20	13 and 17	0.7832	0.7794	0.7790	−4.2	1.40	0.182	1.41	2.19	2.1	0.121	0.94	1.46	4.875	1.33	1.79	Black scale with etched appearance	No scale; thin gray film with a metallic luster on all surfaces
Z-68	21	13 and 17	0.7975	0.7941	0.7935	−4.0	1.40	0.173	1.34	2.08	2.1	0.115	0.89	1.39	5.125	1.24	1.67	Thin oxide film with scale in spots	No scale; thin gray film with a metallic luster on all surfaces
E. Incoloy																			
IN-1	22	13 and 17	0.9853	0.9881	0.9838	−1.5	1.40	0.050	0.39	0.60	2.1	0.033	0.26	0.40	2.625	2.55	3.42	Thin oxide film with scale in spots	Generally clean with a thin brown stain on one side
F. Stainless Steel																			
SE-1	23	13 and 17	0.8837	0.8960	0.8789	−4.8	1.40	0.178	1.38	2.14	2.1	0.118	0.91	1.42	5.625	1.08	1.45	Thin oxide film with scale in spots	Thin dark film on all surfaces
SA-1360A	24	13 and 17	0.9366	0.9418	0.9307	−5.9	1.57	0.184	1.43	2.22	2.1	0.138	1.07	1.66	5.875	1.00	1.34	Scattered flakes of heavy black scale	Clean, slightly etched appearance on all surfaces
G. Titanium																			
TD-1	5	13 and 17	0.4992	0.4988	0.4979	−1.3	1.40	0.081	0.63	0.98	2.1	0.054	0.42	0.65	1.125	3.91	5.25	Very thin black scale	Thin iridescent film on all surfaces
TE-1	6	13 and 17	0.5368	0.5364	0.5352	−1.6	1.40	0.099	0.77	1.19	2.1	0.066	0.51	0.80	1.375	3.65	4.90	Very thin black scale	Thin iridescent film on all surfaces
H. Zircaloy-3																			
ZD-1	7	13 and 17	0.7795	0.7726	0.7718	−7.7	1.40	0.333	2.58	4.01	2.1	0.222	1.72	2.68	1.625	3.40	4.57	Thin brown film on all surfaces	No scale; thin gray film with a metallic luster on all surfaces
ZE-1	8	13 and 17	0.7888	0.7784	0.7815	−7.3	1.40	0.316	2.45	3.81	2.1	0.211	1.63	2.54	1.875	3.17	4.26	Thin black scale in spots	No scale; thin gray film with a metallic luster on all surfaces, with some brown stain
ZF-1	9	13 and 17	0.7853	0.7675	0.7781	−7.2	1.40	0.311	2.41	3.75	2.1	0.207	1.60	2.49	2.125	2.93	3.93	Light-blue oxide film, uniform over all surfaces	No scale; thin gray film with a metallic luster on all surfaces; brown stain on one side
ZG-1	10	13 and 17	0.7899	0.7835	0.7829	−7.0	1.40	0.303	2.35	3.65	2.1	0.202	1.56	2.43	2.375	2.73	3.67	Light-blue oxide film, uniform over all surfaces	No scale; thin gray film with a metallic luster on all surfaces; brown stain on one side
ZI-1	11	13 and 17	0.7900	0.7834	0.7826	−7.4	1.40	0.320	2.48	3.86	2.1	0.213	1.65	2.57	2.625	2.55	3.42	Clean, with brown film on one edge	No scale; thin gray film with a metallic luster on all surfaces, with some brown stain
ZJ-1	12	13 and 17	0.7936	0.7873	0.7867	−6.9	1.40	0.299	2.32	3.60	2.1	0.199	1.54	2.40	2.875	2.38	3.20	Black scale, uniform over all surfaces	No scale; thin gray film with a metallic luster on all surfaces
ZK-1	13	13 and 17	0.7503	0.7384	0.7365	−13.8	1.40	0.596	4.62	7.18	2.1	0.397	3.07	4.78	3.125	2.20	2.95	Etched; light-blue oxide film	No scale; thin gray film with a metallic luster on all surfaces; slightly etched

*Two corrosion rates are presented: one based on the total operation time of 1128 hr and the other based on the total radiation time of 725 hr (3 Mwhr of reactor time equivalent to 1 hr of total radiation time).

Table 21 (continued)

Sample No.	Position	Flow Velocity (fps)	Weight Data: Initial (g)	Weight Data: As Removed (g)	Weight Data: Defilmed (g)	Weight Data: Change (mg)	Exposed Sample Area (cm^2)	Corrosion Penetration (mils)	Corrosion Rate* (Exposed Area) (mpy): 1128 hr	Corrosion Rate* (Exposed Area) (mpy): 725 hr	Total Area (cm^2)	Corrosion Penetration (mils)	Corrosion Rate* (Total Area) (mpy): 1128 hr	Corrosion Rate* (Total Area) (mpy): 725 hr	Distance from Front of First Specimen to Center of Specimen (in.)	Neutron Flux at Specimen Locations (neutrons·cm^{-2}·sec^{-1})	Power Density at Specimen Locations (w/ml)	Appearance: As Removed	Appearance: Defilmed
H. Zircaloy-3																$\times 10^{12}$			
ZL-1	14	13 and 17	0.7682	0.7515	0.7504	−17.8	1.40	0.763	5.91	9.19	2.1	0.509	3.94	6.13	3.375	2.05	2.75	Etched; light-blue oxide film	No scale; thin gray film with a metallic luster on all surfaces; slightly etched
ZM-1	15	13 and 17	0.7736	0.7675	0.7690	−4.6	1.40	0.199	1.54	2.40	2.1	0.133	1.03	1.60	3.625	1.90	2.55	Etched; light-blue oxide film	No scale; thin gray film with a metallic luster on all surfaces
ZN-1	16	13 and 17	0.8258	0.8220	0.8210	−4.8	1.40	0.208	1.61	2.51	2.1	0.139	1.08	1.67	3.875	1.78	2.39	Clean, except scattered flakes of black scale	No scale; thin gray film with a metallic luster on all surfaces
ZO-1	17	13 and 17	0.7584	0.6495	0.6455	−112.9	1.40	4.884	37.83	58.85	2.1	3.256	25.22	39.23	4.125	1.65	2.22	Rough surfaces covered with white chalky powder	Clean after defilming; white chalky appearance returned on standing in air
ZP-1	18	13 and 17	0.7720	0.7817	0.7672	−4.8	1.40	0.208	1.61	2.51	2.1	0.139	1.08	1.67	4.375	1.53	2.05	Thin oxide film; etched appearance	No scale; thin gray film with a metallic luster on all surfaces
ZC-1	19	13 and 17	0.7655	0.7563	0.7545	−11.0	1.40	0.476	3.69	5.74	2.1	0.317	2.46	3.82	4.625	1.43	1.92	Black scale in spots; etched appearance	No scale; thin gray film with a metallic luster on all surfaces, with some brown stain
II. 8 Core Rod Coupon Assemblies (88 Coupons)																			
A. Platinum																			
PT-14	2(A)		1.5192		1.5170	−2.2	3.37	0.012	0.093	0.14	3.83	0.011	0.085	0.13	1.313	3.70	4.97	Dark gray scale, very soft appearance	Bright shiny surfaces
PT-15	5(A)		1.5021		1.4777	−24.4	3.37	0.133	1.03	1.60	3.83	0.117	0.91	1.41	2.413	2.70	3.63	Heavy black film, uniform over all surfaces	Bright shiny surfaces; damaged in removal from rod
PT-16	8(A)		1.5114		1.5063	−5.1	3.37	0.028	0.22	0.34	3.83	0.025	0.19	0.30	3.613	1.91	2.57	Whitish-gray film; on rod there is a heavy black scale broken loose from specimen	Bright shiny surfaces; damaged in removal from rod
B. Alumina																			
Al_2O_3	2(B)		0.7953	0.1666**			3.37				3.83				1.113	3.91	5.25	Very small portion of sample remaining at time of disassembly	
C. Crystal-Bar Zirconium																			
ZZ-13	2(C)		1.3493	1.3404	1.3369	−12.4	3.37	0.223	1.73	2.69	3.83	0.196	1.52	2.36	1.313	3.70	4.97	Flakes of heavy black scale scattered over all surfaces	Thin gray film with a metallic luster; some scattered spots of scale retained
ZZ-14	5(C)		1.3324	1.3172	1.3169	−15.5	3.37	0.279	2.16	3.36	3.83	0.245	1.90	2.95	2.413	2.70	3.63	Clean with some stain on one side	Thin gray film with a metallic luster
ZZ-11	8(C)		1.3516	1.3427	1.3401	−11.5	3.37	0.207	1.60	2.49	3.83	0.182	1.41	2.19	3.613	1.91	2.57	Flakes of brown scale scattered over all surfaces	Thin gray film with a metallic luster
D. Zircaloy-2																			
ZH-25	1(B)		1.2838	1.2670	1.2652	−18.6	3.37	0.334	2.59	4.02	3.83	0.294	2.28	3.54	0.713	4.40	5.91	Metallic bronze color; thin black film in spots	Thin gray film with a metallic luster; brown stains
WC-1	2(D)		1.3453	1.3333	1.3322	−13.1	3.37	0.235	1.82	2.83	3.83	0.207	1.60	2.49	1.113	3.91	5.25	Light-brown film uniformly over all surfaces	Thin gray film with a metallic luster
ZH-9	4(D)		1.3273	1.3142	1.3135	−13.8	3.37	0.248	1.92	2.99	3.83	0.218	1.69	2.63	1.913	3.12	4.19	Light-brown film uniformly over all surfaces	Thin gray film with a metallic luster
WC-3	5(D)		1.3498	1.3349	1.3347	−15.1	3.37	0.271	2.10	3.27	3.83	0.238	1.84	2.87	2.313	2.79	3.75	Light-brown film, with spots of black scale	Thin gray film with a metallic luster
ZH-10	7(D)		1.4016	1.3885	1.3883	−13.3	3.37	0.239	1.85	2.88	3.83	0.210	1.63	2.53	3.113	2.21	2.97	Light-blue stain with two spots of black scale on one side	Thin gray film with a metallic luster
WC-2	8(D)		1.3630	1.3531	1.3516	−11.4	3.37	0.205	1.59	2.47	3.83	0.180	1.39	2.17	3.513	1.98	2.66	Light-blue stain with spots of black scale on one side	Thin gray film with a metallic luster
ZH-11	10(D)		1.3320	1.3225	1.3215	−10.5	3.37	0.189	1.46	2.28	3.83	0.166	1.29	2.00	4.313	1.58	2.12	Clean except for a few spots of stain	Thin gray film with a metallic luster

*Two corrosion rates are presented: one based on the total operation time of 1128 hr and the other based on the total radiotion time of 725 hr (3 Mwhr of reactor time equivalent to 1 hr of total radiation time).

**Broken.

Table 21 (continued)

Sample No.	Position	Flow Velocity (fps)	Weight Data: Initial (g)	Weight Data: As Removed (g)	Weight Data: Defilmed (g)	Weight Data: Change (mg)	Exposed Sample Area (cm^2)	Corrosion Penetration (mils)	Corrosion Rate* (Exposed Area) (mpy): 1128 hr	Corrosion Rate* (Exposed Area) (mpy): 725 hr	Total Area (cm^2)	Corrosion Penetration (mils)	Corrosion Rate* (Total Area) (mpy): 1128 hr	Corrosion Rate* (Total Area) (mpy): 725 hr	Distance from Front of First Specimen to Center of Specimen (in.)	Neutron Flux at Specimen Locations (neutrons·cm^{-2}·sec^{-1})	Power Density at Specimen Locations (w/ml)	Appearance: As Removed	Appearance: Defilmed
D. Zircaloy-2																$\times 10^{12}$			
ZH-2	4(E)		1.3678	1.3527	1.3531	−14.7	3.37	0.264	2.04	3.18	3.83	0.232	1.80	2.80	2.013	3.03	4.07	Clean with a light-bluish color; some brown stain	Thin gray film with a metallic luster
ZH-3	7(E)		1.3323	1.3231	1.3207	−11.6	3.37	0.208	1.61	2.51	3.83	0.183	1.42	2.21	3.213	2.16	2.90	Very thin oxide film; few flakes of scale scattered over surfaces	Thin gray film with a metallic luster; some brown stains
ZH-4	10(E)		1.3530	1.3440	1.3435	−9.5	3.37	0.171	1.32	2.06	3.83	0.150	1.16	1.81	4.413	1.52	2.04	Very thin uniform scale	Thin gray film with a metallic luster
ZH-27	11(F)		1.3608	1.3552	1.3499	−10.9	3.37	0.196	1.52	2.36	3.83	0.172	1.33	2.07	4.713	1.40	1.88	Clean with scattered flakes of scale over all surfaces	Thin gray film with a metallic luster; one edge slightly etched
E. Incoloy																			
IN-12	4(F)		1.6343	1.6299	1.6018	−32.5	3.37	0.446	3.45	5.37	3.83	0.392	3.04	4.72	1.913	3.12	4.19	Heavy black scale that is thin in spots	Clean metallic surfaces with brown stain on one side
IN-13	7(F)		1.6720	1.6841	1.6676	−4.4	3.37	0.060	0.46	0.72	3.83	0.053	0.41	0.64	3.113	2.21	2.97	Gun-metal blue in appearance with black flakes of scale	Clean metallic surfaces
IN-11	10(F)		1.6363	1.6644	1.6349	−1.4	3.37	0.019	0.15	0.23	3.83	0.017	0.13	0.20	4.313	1.58	2.12	Black velvety film over all surfaces	Clean metallic surfaces
F. Stainless Steel																			
SF-2	11(B)		1.3309	1.3941	1.3294	−1.5	3.37	0.023	0.18	0.28	3.83	0.020	0.15	0.24	4.713	1.40	1.88	Heavy black velvety film over all surfaces	Clean metallic surfaces; machine marks visible
SG-14	11(C)		1.7077	1.7287	1.7066	−1.1	3.37	0.017	0.13	0.20	3.83	0.015	0.12	0.18	4.813	1.36	1.83	Block oxide scale, flaked off in places	Clean metallic surfaces; machine marks visible
SF-1	1(F)		1.3200	1.2504	1.2346	−85.4	3.37	1.313	10.17	15.82	3.83	1.155	8.95	13.92	0.713	4.40	5.91	Black thin film which is heavy in spots	Clean metallic surfaces; machine marks visible
SG-13	1(G)		1.7170	1.7147	1.7050	−12.0	3.37	0.184	1.43	2.22	3.83	0.162	1.25	1.94	0.913	4.17	5.60	Very thin brown film	Clean metallic surfaces; machine marks visible
SE-9	7(G)		1.5520	1.6003	1.5519	−0.1	3.37	0.002	0.02	0.02	3.83	0.001	0.001	0.008	3.213	2.16	2.90	Heavy black scale over all surfaces	Clean metallic surfaces; machine marks visible
SE-10	4(G)		1.5320	1.5319	1.5270	−5.0	3.37	0.077	0.60	0.93	3.83	0.068	0.53	0.82	2.013	3.03	4.07	Scattered flakes of black scale; specimen is a light gray in color	Thin light-gray film retained on all surfaces; machine marks visible
SE-12	10(G)		1.5541	1.5921	1.5540	−0.1	3.37	0.002	0.02	0.02	3.83	0.001	0.01	0.02	4.413	1.52	2.04	Heavy black scale over all surfaces	Thin light-gray film retained on all surfaces; machine marks visible
SA-1262A	4(H)		1.6510		1.6440	−7.0	3.37	0.102	0.79	1.23	3.83	0.090	0.70	1.08	1.913	3.12	4.19	Rust-red scale uniformly over all surfaces	Clean metallic surfaces; machine marks visible
SA-1273A	7(H)		1.6547	1.6753	1.6534	−1.3	3.37	0.019	0.15	0.23	3.83	0.017	0.13	0.20	3.113	2.21	2.97	Heavy black scale, uniform over all surfaces	Clean metallic surfaces; machine marks visible
SA-1270A	10(H)		1.6498	1.6808	1.6488	−1.0	3.37	0.015	0.12	0.18	3.83	0.013	0.10	0.16	4.313	1.58	2.12	Heavy black scale, velvety in appearance	Clean metallic surfaces; machine marks visible
G. Titanium																			
TB-1481A	5(B)		0.9212	0.9215	0.9198	−1.4	3.37	0.036	0.28	0.43	3.83	0.032	0.25	0.39	2.313	2.79	3.75	Clean with a flake of scale on one side	Thin iridescent film on all surfaces
TB-1477A	8(B)		0.9416	0.9414	0.9410	−0.4	3.37	0.010	0.08	0.12	3.83	0.009	0.07	0.11	3.513	1.98	2.66	Clean except for a few spots of black scale on both sides	Thin iridescent film on all surfaces
TD-12	2(E)		0.9353	0.9342	0.9336	−1.7	3.37	0.044	0.34	0.53	3.83	0.039	0.30	0.47	1.313	3.70	4.97	Metallic bronze color with scattered flakes of film	Thin iridescent film on all surfaces
TD-14	5(E)		0.8305	0.9315	0.9297	−0.7	3.37	0.018	0.14	0.22	3.83	0.016	0.12	0.19	2.413	2.70	3.63	Thin oxide film, metallic bronze in color, with scattered spots of scale	Thin iridescent film on all surfaces

*Two corrosion rates are presented: one based on the total operation time of 1128 hr and the other based on the total radiation time of 725 hr (3 Mwhr of reactor time equivalent to 1 hr of total radiation time).

Table 21 (continued)

Sample No.	Position	Flow Velocity (fps)	Weight Data: Initial (g)	Weight Data: As Removed (g)	Weight Data: Defilmed (g)	Weight Data: Change (mg)	Exposed Sample Area (cm^2)	Corrosion Penetration (mils)	Corrosion Rate* (Exposed Area) (mpy): 1128 hr	Corrosion Rate* (Exposed Area) (mpy): 725 hr	Total Area (cm^2)	Corrosion Penetration (mils)	Corrosion Rate* (Total Area) (mpy): 1128 hr	Corrosion Rate* (Total Area) (mpy): 725 hr	Distance from Front of First Specimen to Center of Specimen (in.)	Neutron Flux at Specimen Locations (neutrons·cm^{-2}·sec^{-1})	Power Density at Specimen Locations (w/ml)	Appearance: As Removed	Appearance: Defilmed
G. Titanium																$\times 10^{12}$			
TD-13	8(E)		0.9310	0.9690	0.9311	+0.1	3.37				3.83				3.613	1.91	2.57	Heavy black scale on surface; edges bare	Thin iridescent film on all surfaces
TE-12	2(F)		0.9301	0.9302	0.9280	−2.1	3.37	0.054	0.42	0.65	3.83	0.048	0.37	0.58	1.113	3.91	5.25	Metallic bronze color; scattered flakes of black scale	Thin iridescent film on all surfaces
TE-14	5(F)		0.9391	0.9397	0.9375	−1.6	3.37	0.041	0.32	0.49	3.83	0.036	0.28	0.43	2.313	2.79	3.75	Metallic bronze color; scattered flakes of black scale	Thin iridescent film on all surfaces
TE-15	8(F)		0.8855	0.9274	0.8824	−3.1	3.37	0.080	0.62	0.96	3.83	0.070	0.54	0.84	3.513	1.98	2.66	Heavy black scale flakes; rust-red in bare spots	Thin iridescent film on all surfaces
H. Zircaloy-3																			
ZT-1	1(A)		1.4017	1.3960	1.3958	−5.9	3.37	0.101	0.78	1.22	3.83	0.089	0.69	1.07	0.913	4.17	5.60	Light-purplish oxide film with a few flakes of black film	Very thin oily-appearing film speckled over the entire surface
ZF-7	3(A)		1.3717		1.3580	−13.7	3.37	0.246	1.91	2.96	3.83	0.216	1.67	2.60	1.713	3.30	4.43	Heavy black film, uniform on all surfaces	Thin gray film with a metallic luster; slightly scarred on removal
ZO-11	4(A)		1.3356		1.0183	−317.3	3.37	5.703	44.17	68.72	3.83	5.018	38.86	60.47	2.013	3.03	4.07	Dark gray scale, very soft in appearance and uniform over all surfaces	Uniformly etched surfaces; clean on defilming; chalky powder reforms on air exposure
ZF-9	6(A)		1.3782		1.3660	−13.2	3.37	0.237	1.84	2.86	3.83	0.209	1.62	2.52	2.813	2.41	3.24	Heavy brown scale, uniform over all surfaces	Thin dark-blue film with a metallic luster
ZO-12	7(A)		1.3367		1.0570	−279.7	3.37	5.027	38.93	60.57	3.83	4.423	34.25	53.30	3.213	2.16	2.90	Dark gray scale, very soft in appearance, uniform over all surfaces	Uniformly etched surfaces; clean on defilming; chalky powder reforms on air exposure
ZF-8	9(A)		1.3759		1.3673	−8.6	3.37	0.155	1.20	1.87	3.83	0.136	1.05	1.64	4.013	1.71	2.30	Specimen has a band of whitish-gray film; remainder of specimen covered with soft black film	Thin gray film with a metallic luster; some spots of brown stain
ZO-8	10(A)		1.3278		0.7667	−561.1	3.37	10.084	78.10	121.51	3.83	8.873	68.72	106.92	4.413	1.52	2.04	Has a white-gray film over all surfaces, powdery in appearance	Etched and pitted surfaces; clean on defilming; chalky powder reforms on air exposure
ZS-10	11(A)		1.3493	1.3404	1.3409	−8.4	3.37	0.151	1.17	1.82	3.83	0.133	1.03	1.60	4.813	1.36	1.83	Light-purplish oxide film	Thin dark film with a metallic luster; some spots of brown stain
ZG-12	3(B)		1.3773	1.3680	1.3623	−15.0	3.37	0.270	2.09	3.25	3.83	0.238	1.84	2.87	1.513	3.50	4.70	Light blue in appearance; some stain on surfaces	Thin gray film with a metallic luster
ZP-16	4(B)		1.3213	1.3060	1.3045	−16.8	3.37	0.302	2.34	3.64	3.83	0.266	2.06	3.21	1.913	3.12	4.19	Clean with rust-red stain over all surfaces	Thin gray film with a metallic luster
ZG-14	6(B)		1.3466	1.3340	1.3328	−13.8	3.37	0.248	1.92	2.99	3.83	0.218	1.69	2.63	2.713	2.48	3.33	Light blue in appearance; one corner covered with reddish-brown scale	Thin gray film with a metallic luster
ZP-13	7(B)		1.3034	1.2902	1.2901	−13.3	3.37	0.239	1.85	2.88	3.83	0.210	1.63	2.53	3.113	2.21	2.97	Clean in appearance with a few spots of black scale on both sides	Thin gray film with a metallic luster
ZG-18	9(B)		1.3746	1.3648	1.3642	−10.4	3.37	0.187	1.45	2.25	3.83	0.165	1.28	1.99	3.913	1.77	2.38	Clean with stain on both sides	Thin gray film with a metallic luster
ZP-15	10(B)		1.3280	1.3179	1.3170	−11.0	3.37	0.198	1.53	2.39	3.83	0.174	1.35	2.10	4.313	1.58	2.12	Clean except for a few spots of black scale on both sides	Thin gray film with a metallic luster
ZQ-2	1(C)		1.3356	1.3196	1.3191	−16.5	3.37	0.297	2.30	3.58	3.83	0.261	2.02	3.14	0.913	4.17	5.60	Flaky brown scale over all surfaces	Thin gray film with a metallic luster
ZI-12	3(C)		1.3726	1.3586	1.3556	−17.0	3.37	0.306	2.37	3.69	3.83	0.269	2.08	3.24	1.713	3.30	4.43	Flakes of heavy black scale scattered over all surfaces	Thin gray film with a metallic luster; some spots of scale retained
ZC-10	4(C)		1.3298	1.2954	1.2919	−37.9	3.37	0.681	5.27	8.21	3.83	0.599	3.86	7.22	2.013	3.03	4.07	Thin gray film with scattered flakes of black scale	Thin gray film with a metallic luster; surface generally roughened
ZI-13	6(C)		1.3663	1.3499	1.3501	−16.2	3.37	0.291	2.25	3.51	3.83	0.256	1.98	3.08	2.813	2.41	3.24	Light gray in appearance with flakes of brown scattered over all surfaces	Thin gray film with a metallic luster

*Two corrosion rates are presented: one based on the total operation time of 1128 hr and the other based on the total radiation time of 725 hr (3 Mwhr of reactor time equivalent to 1 hr of total radiation time).

Table 21 (continued)

Sample No.	Position	Flow Velocity (fps)	Weight Data: Initial (g)	Weight Data: As Removed (g)	Weight Data: Defilmed (g)	Weight Data: Change (mg)	Exposed Sample Area (cm^2)	Corrosion Penetration (mils)	Corrosion Rate* (Exposed Area) (mpy): 1128 hr	Corrosion Rate* (Exposed Area) (mpy): 725 hr	Total Area (cm^2)	Corrosion Penetration (mils)	Corrosion Rate* (Total Area) (mpy): 1128 hr	Corrosion Rate* (Total Area) (mpy): 725 hr	Distance from Front of First Specimen to Center of Specimen (in.)	Neutron Flux at Specimen Locations (neutrons·cm^{-2}·sec^{-1})	Power Density at Specimen Locations (w/ml)	Appearance: As Removed	Appearance: Defilmed
H. Zircaloy-3																$\times 10^{12}$			
ZC-9	7(C)		1.3267	1.3009	1.2934	−33.3	3.37	0.598	4.63	7.21	3.83	0.526	4.07	6.34	3.213	2.16	2.90	Heavy flakes of film scattered over all surfaces	Thin gray film with a metallic luster; slightly etched surfaces
ZI-14	9(C)		1.3410	1.3292	1.3278	−13.2	3.37	0.237	1.84	2.86	3.83	0.209	1.62	2.52	4.013	1.71	2.30	Clean except for few flakes of scale on edges	Thin gray film with a metallic luster
ZC-7	10(C)		1.3375	1.3215	1.3171	−20.4	3.37	0.367	2.84	4.42	3.83	0.323	2.50	3.89	4.413	1.52	2.04	Light red in appearance with brown scale scattered over all surfaces	Thin gray film with a metallic luster; slightly etched surfaces
ZR-1	1(D)		1.3712	1.3559	1.3536	−17.6	3.37	0.316	2.45	3.81	3.83	0.278	2.15	3.35	0.713	4.40	5.91	Light-brown film, uniform over all surfaces	Thin gray film with a metallic luster
ZJ-14	3(D)		1.3622	1.3473	1.3458	−16.4	3.37	0.295	2.28	3.55	3.83	0.260	2.01	3.13	1.513	3.50	4.70	Light-brown film, uniform over all surfaces	Thin gray film with a metallic luster
ZJ-15	6(D)		1.3735	1.3592	1.3583	−15.2	3.37	0.273	2.11	3.29	3.83	0.240	1.86	2.89	2.713	2.48	3.33	Clean in appearance with same stain on specimen	Thin gray film with a metallic luster; some brown stain on one side
ZJ-13	9(D)		1.3713	1.3614	1.3599	−11.4	3.37	0.205	1.59	2.47	3.83	0.180	1.39	2.17	3.913	1.77	2.38	Light-blue stain with two spots of film on one side	Thin gray film with a metallic luster
ZU-1	11(D)		1.3783	1.3638	1.3618	−16.5	3.37	0.294	2.28	3.54	3.83	0.259	2.01	3.12	4.713	1.40	1.88	Black oxide scale, flaked off in places	Thin gray film with a metallic luster
ZS-9	1(E)		1.3710	1.3547	1.3549	−16.1	3.37	0.289	2.24	3.48	3.83	0.254	1.97	3.06	0.913	4.17	5.60	Light gray in appearance with same scale on edges	Thin gray film with a metallic luster
ZK-12	3(E)		1.3177	1.2791	1.2784	−39.3	3.37	0.706	5.47	8.51	3.83	0.621	4.81	7.48	1.713	3.30	4.43	Very thin brown oxide film	Thin gray film with a metallic luster
ZK-11	6(E)		1.2990	1.2700	1.2685	−30.5	3.37	0.548	4.24	6.60	3.83	0.482	3.73	5.81	2.813	2.41	3.24	Patches of scale; otherwise clean	Thin gray film with a metallic luster; slightly etched surfaces
ZK-14	9(E)		1.3138	1.3036	1.2920	−21.8	3.37	0.392	3.04	4.72	3.83	0.345	2.67	4.16	4.013	1.71	2.30	Heavy black scale, uniform over all surfaces	Thin black film on all surfaces; all surfaces slightly etched
ZT-2	11(E)		1.4218	1.4268	1.4218	0.0	3.37	0.0	0.0	0.0	3.83	0.0	0.0	0.0	4.813	1.36	1.83	Black thin scale, uniform over all surfaces	Very thin oily-appearing film speckled over all surfaces
ZL-11	3(F)		1.3302	1.2874	1.2863	−43.9	3.37	0.789	6.11	9.51	3.83	0.694	5.37	8.36	1.513	3.50	4.70	Light gray in color with spots of black film	Thin black film on all surfaces
ZL-13	6(F)		1.3184	1.2852	1.2831	−35.3	3.37	0.634	4.91	7.64	3.83	0.558	4.32	6.72	2.713	2.48	3.33	Gun-metal blue in appearance with scattered black flakes of scale	Thin black film on all surfaces
ZL-12	9(F)		1.3227	1.2969	1.2945	−28.2	3.37	0.506	3.92	4.89	3.83	0.445	3.45	5.36	3.913	1.77	2.38	Light gray in color; flakes of brown scale scattered over all surfaces	Thin black film on all surfaces
ZD-7	2(G)		1.2157	1.1989	1.1979	−17.8	3.37	0.320	2.48	3.86	3.83	0.282	2.18	3.40	1.313	3.70	4.97	Very thin loose brown film	Thin gray film with a metallic luster
ZM-13	3(G)		1.3392	1.3226	1.3228	−16.4	3.37	0.294	2.28	3.54	3.83	0.259	2.01	3.12	1.713	3.30	4.43	Clean in appearance with spots of black stain	Thin gray film with a metallic luster
ZD-8	5(G)		1.2940	1.2789	1.2791	−14.9	3.37	0.268	2.08	3.23	3.83	0.236	1.83	2.84	2.413	2.70	3.63	Clean in appearance with a few flakes of scattered black scale	Thin gray film with a metallic luster
ZM-11	6(G)		1.3507	1.3430	1.3392	−11.5	3.37	0.207	1.60	2.49	3.83	0.182	1.41	2.19	2.813	2.41	3.24	Light-blue color; flakes of black scale over both sides	Thin gray film with a metallic luster
ZD-9	8(G)		1.1997	1.1928	1.1895	−10.2	3.37	0.183	1.42	2.21	3.83	0.161	1.25	1.94	3.613	1.91	2.57	Gray in appearance with patches of heavy scale	Thin gray film with a metallic luster
ZM-14	9(G)		1.3398	1.3330	1.3302	−9.6	3.37	0.173	1.34	2.08	3.83	0.152	1.18	1.83	4.013	1.71	2.30	Clean except for loose brown stain scattered over area	Thin gray film with a metallic luster
ZQ-1	11(G)		1.3257	1.3205	1.3180	−7.7	3.37	0.138	1.07	1.66	3.83	0.121	0.94	1.46	4.813	1.36	1.83	Light gray in color; flakes of brown scale over all areas	Thin gray film with a metallic luster; small brown stain
ZU-2	1(H)		1.4043	1.3832	1.3821	−22.2	3.37	0.395	3.06	4.76	3.83	0.348	2.70	4.19	0.713	4.40	5.91	Thin rust-red film over all surfaces	Thin gray film with a metallic luster

*Two corrosion rates are presented: one based on the total operation time of 1128 hr and the other based on the total radiation time of 725 hr (3 Mwhr of reactor time equivalent to 1 hr of total radiation time).

Table 21 (continued)

Sample No.	Position	Flow Velocity (fps)	Weight Data: Initial (g)	Weight Data: As Removed (g)	Weight Data: Defilmed (g)	Weight Data: Change (mg)	Exposed Sample Area (cm^2)	Corrosion Penetration (mils)	Corrosion Rate* (Exposed Area) (mpy): 1128 hr	Corrosion Rate* (Exposed Area) (mpy): 725 hr	Total Area (cm^2)	Corrosion Penetration (mils)	Corrosion Rate* (Total Area) (mpy): 1128 hr	Corrosion Rate* (Total Area) (mpy): 725 hr	Distance from Front of First Specimen to Center of Specimen (in.)	Neutron Flux at Specimen Locations (neutrons·cm^{-2}·sec^{-1})	Power Density at Specimen Locations (w/ml)	Appearance: As Removed	Appearance: Defilmed
H. Zircaloy-3																$\times 10^{12}$			
ZE-6	2(H)		1.3367	1.3219	1.3199	−16.8	3.37	0.302	2.34	3.64	3.83	0.266	2.06	3.21	1.113	3.91	5.25	Thin rust-red film over all surfaces	Thin gray film with a metallic luster
ZN-14	3(H)		1.4082	1.3979	1.3956	−12.6	3.37	0.226	1.75	2.72	3.83	0.199	1.54	2.40	1.513	3.50	4.70	Clean with scattered spots of soft black scale	Thin gray film with a metallic luster; small brown stain
ZE-9	5(H)		1.3156		1.3012	−14.4	3.37	0.259	2.01	3.12	3.83	0.228	1.77	2.75	2.313	2.79	3.75	Rust-red scale, uniform over all surfaces	Thin gray film with a metallic luster
ZN-12	6(H)		1.3517	1.3418	1.3401	−11.6	3.37	0.208	1.61	2.51	3.83	0.183	1.42	2.21	2.713	2.48	3.33	Clean in appearance with spots of black scale scattered over surface	Thin gray film with a metallic luster
ZE-8	8(H)		1.3485	1.3392	1.3374	−11.1	3.37	0.199	1.54	2.40	3.83	0.175	1.36	2.11	3.513	1.98	2.66	Very thin red oxide film; flakes of black scale	Thin gray film with a metallic luster
ZN-11	9(H)		1.3627	1.3560	1.3536	−9.1	3.37	0.164	1.27	1.98	3.83	0.144	1.12	1.74	3.913	1.77	2.38	Very thin red oxide film with flakes of black scale scattered over area	Thin gray film with a metallic luster
ZR-2	11(H)		1.2936	1.2872	1.2855	−8.1	3.37	0.146	1.13	1.76	3.83	0.128	0.99	1.54	4.713	1.40	1.88	Rust-red in color; very thin oxide scale	Thin gray film with a metallic luster
III. 24 In-Line Corrosion Sample Coupons																			
A. Platinum																			
PT-11	1	13 and 17	2.5308	2.5358	2.5309	+0.1	1.57				2.1				0.125			Dark, heavy black scale, uniform over all surfaces	Bright, heavy surfaces with some flakes of scale retained on the edges
B. Alumina (Notched)																			
Al_2O_3	2	13 and 17	0.4577				1.40				2.1				0.375			(Specimen disintegrated)	
C. Crystal-Bar Zirconium																			
ZZ-2	3	13 and 17	0.7724	0.7764	0.7726	+0.2	1.40				2.1				0.625			Dark, heavy black scale, uniform over all surfaces	Thin gray film with a metallic luster; some scale retained in clamping areas
D. Zircaloy-2																			
WB-2	4	13 and 17	0.7975	0.8030	0.7983	+0.8	1.40				2.1				0.875			Heavy black scale, flaked off in spots on both sides	Thin gray film with a metallic luster; some scale retained in clamping areas
Z-51	20	13 and 17	0.7744	0.7831	0.7762	+1.8	1.40				2.1				4.875			Thin blue scale, uniform over all surfaces	Thin iridescent film with a metallic luster; some scale retained in clamping areas
Z-69	21	13 and 17	0.7886	0.7940	0.7895	+0.9	1.40				2.1				5.125			Thin blue scale, uniform over all surfaces	Thin iridescent film with a metallic luster; some scale retained in clamping areas
E. Incoloy																			
IN-2	22	13 and 17	0.9562	0.9652	0.9560	−0.2	1.40	0.007	0.05	0.08	2.1	0.005	0.04	0.06	2.625			Thin blue scale, uniform over all surfaces	Thin gray film on all surfaces; some scale retained in clamping areas
F. Stainless Steel																			
SE-2	23	13	0.9047	0.9139	0.8994	−5.3	1.40	0.196	1.52	2.36	2.1	0.131	1.01	1.58	5.625			Thin blue scale, uniform over all surfaces	Thin sooty-black film on all surfaces
SA-2	24	13 and 17	0.9531	0.9622	0.9524	−0.7	1.40	0.022	0.17	0.27	2.1	0.016	0.12	0.19	5.875			Thin blue scale, uniform over all surfaces	Very thin dark film on all surfaces
G. Titanium																			
TD-2	5	13	0.4888	0.4974	0.4876	−1.2	1.40	0.074	0.57	0.89	2.1	0.049	0.38	0.59	1.125			Heavy black film, uniform over all surfaces; rust-red on edges	Thin iridescent film on all surfaces
TE-2	6	13	0.5306	0.5388	0.5289	−1.7	1.40	0.105	0.81	1.27	2.1	0.700	5.42	8.43	1.375			Heavy black film, uniform over all surfaces; rust-red on edges	Thin iridescent film on all surfaces

*Two corrosion rates are presented: one based on the total operation time of 1128 hr and the other based on the total radiation time of 725 hr (3 Mwhr of reactor time equivalent to 1 hr of total radiation time).

Table 21 (continued)

Sample No.	Position	Flow Velocity (fps)	Weight Data: Initial (g)	Weight Data: As Removed (g)	Weight Data: Defilmed (g)	Weight Data: Change (mg)	Exposed Sample Area (cm^2)	Corrosion Penetration (mils)	Corrosion Rate* (Exposed Area) (mpy): 1128 hr	Corrosion Rate* (Exposed Area) (mpy): 725 hr	Total Area (cm^2)	Corrosion Penetration (mils)	Corrosion Rate* (Total Area) (mpy): 1128 hr	Corrosion Rate* (Total Area) (mpy): 725 hr	Distance from Front of First Specimen to Center of Specimen (in.)	Neutron Flux at Specimen Locations (neutrons·cm^{-2}·sec^{-1})	Power Density at Specimen Locations (w/ml)	Appearance: As Removed	Appearance: Defilmed
H. Zircaloy-3																			
ZD-2	7	13 and 17	0.7588	0.7704	0.7598	+1.0	1.40				2.1				1.625			Heavy black uniform scale over all surfaces	Thin iridescent film with metallic luster; some scale in clamping areas
ZE-2	8	13 and 17	0.7535	0.7647	0.7541	+0.6	1.40				2.1				1.875			Heavy black uniform scale over all surfaces	Thin iridescent film with metallic luster; some scale in clamping areas
ZF-2	9	13 and 17	0.7497	0.7542	0.7503	+0.6	1.40				2.1				2.125			Heavy black uniform scale over all surfaces	Thin iridescent film with metallic luster; some scale in clamping areas
ZG-2	10	13 and 17	0.7931	0.7980	0.7937	+0.6	1.40				2.1				2.375			Heavy black scale, flaked off in places on both sides	Thin iridescent film with metallic luster; some scale in clamping areas
ZI-2	11	13 and 17	0.7814	0.7950	0.7822	+0.8	1.40				2.1				2.625			Heavy black scale, uniform over all surfaces	Thin iridescent film with metallic luster on all surfaces
ZJ-2	12	13 and 17	0.7922	0.8015	0.7934	+1.2	1.40				2.1				2.875			Heavy black scale, flaked off in places on both sides	Thin iridescent film with metallic luster on all surfaces
ZK-2	13	13 and 17	0.7724	0.7777	0.7754	+3.0	1.40				2.1				3.125			Heavy, black, uniform scale over all surfaces	Thin iridescent film with metallic luster on edges
ZL-2	14	13 and 17	0.7652	0.7739	0.7672	+2.0	1.40				2.1				3.375			Heavy black scale, uniform over all surfaces	Thin iridescent film with metallic luster on edges
ZM-2	15	13 and 17	0.7725	0.7773	0.7732	+0.7	1.40				2.1				3.625			Rose-colored thin film over all surfaces	Thin iridescent film with metallic luster; very heavy scale along one edge
ZN-2	16	13 and 17	0.7928	0.8008	0.7950	+2.2	1.40				2.1				3.875			Heavy scale on edges, flaked off on sides	Thin iridescent film with metallic luster; some flakes of scale along edges
ZO-2	17	13 and 17	0.7688	0.6780	0.6554	−113.4	1.40	4.906	38.00	59.12	2.1	3.270	25.32	39.40	4.125			Uniform white chalky appearance with scattered flakes of brown scale	Very heavy attack in flow regions; clamping areas partially protected; chalky-powder edges
ZP-2	18	13 and 17	0.7788	0.7816	0.7797	+0.9	1.40				2.1				4.375			Spots of brown scale scattered over all surfaces; machine marks visible	Thin iridescent film with a metallic luster; some scale in clamping areas
ZC-2	19	13 and 17	0.7668	0.7610	0.7572	−9.6	1.40	0.415	3.21	5.00	2.1	0.277	2.15	3.34	4.625			Clean except for one spot of brown film on one side	Thin layer of chalky powder on all surfaces
IV. 4 Line Rod Coupon Assemblies (40 Coupons)																			
A. Platinum																			
PT-17	1(J)		1.4501	1.4602	1.4501	0.0	3.37	0.0	0.0	0.0	3.83	0.0	0.0	0.0				Heavy uniform brown scale over all surfaces	Bright metallic surfaces; some scale retained inside center hole
B. Crystal-Bar Zirconium																			
ZZ-12	1(L)		1.3252	1.3422	1.3296	+4.4	3.37				3.83							Heavy rust-red scale, uniform over all surfaces	
C. Zircaloy-2																			
ZH-13	7(K)		1.3973	1.4161	1.4001	+2.8	3.37				3.83							Heavy rust-red scale, uniform over all surfaces	Thin gray film with a metallic luster; some scattered flakes of scale
ZH-5	7(L)		1.3038	1.3217	1.3048	+1.0	3.37											Light-blue oxide scale; one side has a spot of brown film	Thin gray film with a metallic luster; some scattered flakes of scale
ZH-31	2(M)		1.2693	1.2881	1.2716	+2.3	3.37				3.83							Heavy rust-red scale uniformly over all surfaces	Thin blue film with a metallic luster; some scattered flakes of scale

*Two corrosion rates are presented: one based on the total operation time of 1128 hr and the other based on the total radiation time of 725 hr (3 Mwhr of reactor time equivalent to 1 hr of total radiation time).

Table 21 (continued)

Sample No.	Position	Flow Velocity (fps)	Weight Data: Initial (g)	Weight Data: As Removed (g)	Weight Data: Defilmed (g)	Weight Data: Change (mg)	Exposed Sample Area (cm^2)	Corrosion Penetration (mils)	Corrosion Rate* (Exposed Area) (mpy): 1128 hr	Corrosion Rate* (Exposed Area) (mpy): 725 hr	Total Area (cm^2)	Corrosion Penetration (mils)	Corrosion Rate* (Total Area) (mpy): 1128 hr	Corrosion Rate* (Total Area) (mpy): 725 hr	Distance from Front of First Specimen to Center of Specimen (in.)	Neutron Flux at Specimen Locations (neutrons·cm^{-2}·sec^{-1})	Power Density at Specimen Locations (w/ml)	Appearance: As Removed	Appearance: Defilmed
D. Incoloy																			
IN-14	8(J)		1.6180	1.6367	1.6174	−0.6	3.37	0.008	0.06	0.10	3.83	0.007	0.05	0.08				Heavy uniform brown scale over all surfaces	Clean metallic surfaces with some brown stains
E. Stainless Steel																			
SA-1272A	10(J)		1.6249	1.6455	1.6247	+0.2	3.37				3.83							Heavy brown scale, uniform over all surfaces	Clean metallic surfaces with some brown stains
SE-11	8(K)		1.5546	1.5716	1.5548	+0.2	3.37				3.83							Heavy rust-red scale with one white spot on one side	Clean metallic surfaces with some brown stains
SA-1265A	10(K)		1.6517	1.6700	1.6524	+0.7	3.37				3.83							Heavy rust-red scale, uniform over all surfaces	Clean metallic surfaces with some brown stains
SA-1271A	8(L)		1.6659	1.6842	1.6661	+0.2	3.37				3.83							Heavy rust-red scale, uniform over all surfaces	Clean metallic surfaces with some brown stains
SA-1269A	10(L)		1.6530	1.6724	1.6539	+0.9	3.37				3.83							Heavy rust-red scale, uniform over all surfaces	Clean metallic surfaces with some brown stains and scale on edges
SF-3	6(M)		1.2971	1.3138	1.2959	−1.2	3.37	0.019	0.15	0.23	3.83	0.017	0.13	0.20				Heavy rust-red scale, uniform over all surfaces	Clean metallic surfaces with some scale retained on edges
SG-15	7(M)		1.7125	1.7311	1.7120	−0.5	3.37	0.008	0.06	0.10	3.83	0.007	0.05	0.08				Heavy rust-red scale, uniform over all surfaces	Clean metallic surfaces with some brown stains
SA-1266A	10(M)		1.6514	1.6714	1.6508	−0.9	3.37	0.014	0.11	0.17	3.83	0.012	0.09	0.14				Heavy rust-red scale, uniform over all surfaces	Clean metallic surfaces with some brown stains
F. Titanium																			
TB-1483A	2(J)		0.9052	0.9372	0.9041	−1.1	3.37	0.028	0.22	0.34	3.83	0.025	0.19	0.30				Heavy brown scale, uniform over all surfaces	Thin blue film on all surfaces, with scattered spots of scale
TB-1478A	9(J)		0.9301	0.9533	0.9299	−0.2	3.37	0.005	0.04	0.06	3.83	0.004	0.03	0.05				Heavy brown scale, uniform over all surfaces	Thin blue film on all surfaces, with some brown stains
TB-1484A	1(K)		0.9315	0.9463	0.9316	+0.1	3.37				3.83							Heavy rust-red scale, uniform over all surfaces	Thin blue film on all surfaces, with some brown stains
TD-11	2(K)		0.8977	0.9115	0.8980	+0.3	3.37				3.83							Heavy rust-red scale, uniform over all surfaces	Thin blue film on all surfaces, with scattered spots of scale
TB-1475A	9(K)		0.9312	0.9518	0.9260	−5.2	3.37	0.134	1.04	1.61	3.83	0.118	9.14	14.22				Heavy rust-red scale, uniform over all surfaces	Thin blue film on all surfaces
TE-13	2(L)		0.8918	0.9056	0.8905	−1.3	3.37	0.033	0.26	0.40	3.83	0.029	0.22	0.35				Heavy rust-red scale, uniform over all surfaces	Thin blue film on all surfaces, with some brown stains
TB-1474A	9(L)		0.9393	0.9568	0.9378	−1.5	3.37	0.038	0.29	0.46	3.83	0.033	0.26	0.40				Heavy rust-red scale, uniform over all surfaces	Thin blue film on all surfaces, with some brown stains
TB-1480A	9(M)		0.9317	0.9531	0.9252	−6.5	3.37	0.165	1.28	1.99	3.83	0.145	1.12	1.75				Heavy rust-red scale, uniform over all surfaces	Thin blue film on all surfaces, with some brown stains
G. Zircaloy-3																			
ZD-10	3(J)		1.1704	1.1941	1.1714	+1.0	3.37				3.83							Heavy brown scale, uniform over all surfaces	Thin dark film on all surfaces, with scattered flakes of scale
ZG-11	4(J)		1.3340	1.3508	1.3354	+1.4	3.37				3.83							Heavy rust-red scale, flaked off in spots; light blue underneath	Thin dark film on all surfaces, with scattered flakes of scale

*Two corrosion rates are presented: one based on the total operation time of 1128 hr and the other based on the total radiation time of 725 hr (3 Mwhr of reactor time equivalent to 1 hr of total radiation time).

Table 21 (continued)

Sample No.	Position	Flow Velocity (fps)	Weight Data: Initial (g)	Weight Data: As Removed (g)	Weight Data: Defilmed (g)	Weight Data: Change (mg)	Exposed Sample Area (cm^2)	Corrosion Penetration (mils)	Corrosion Rate* (Exposed Area) (mpy): 1128 hr	Corrosion Rate* (Exposed Area) (mpy): 725 hr	Total Area (cm^2)	Corrosion Penetration (mils)	Corrosion Rate* (Total Area) (mpy): 1128 hr	Corrosion Rate* (Total Area) (mpy): 725 hr	Distance from Front of First Specimen to Center of Specimen (in.)	Neutron Flux at Specimen Locations (neutrons·cm^{-2}·sec^{-1})	Power Density at Specimen Locations (w/ml)	Appearance: As Removed	Appearance: Defilmed
G. Zircaloy-3																$\times 10^{12}$			
ZK-13	5(J)		1.3036	1.3195	1.3060	+2.4	3.37				3.83							Heavy rust-red scale, flaked off in spots; light blue underneath	Thin dark film on all surfaces, with scattered flakes of scale
ZN-13	6(J)		1.3342	1.3541	1.3355	+1.3	3.37				3.83							Heavy rust-red scale, flaked off; light blue underneath	Thin blue film on all surfaces, with scattered flakes of scale
ZC-8	7(J)		1.3106	1.3090	1.2965	−14.1	3.37	0.253	1.96	3.05	3.83	0.223	1.73	2.69				One side clean; other side has a heavy rust-red film	Thin gray film on all surfaces, with scattered flakes of scale; general etched appearance
ZE-7	3(K)		1.2878	1.3068	1.2882	+0.4	3.37				3.83							Heavy rust-red scale, uniform over all surfaces	Thin blue film on all surfaces
ZI-11	4(K)		1.3610	1.3796	1.3611	+0.1	3.37				3.83							Heavy rust-red scale, uniform over all surfaces	Thin blue film on all surfaces, with scattered flakes of scale
ZL-14	5(K)		1.3112	1.3252	1.3134	+2.2	3.37				3.83							Heavy rust-red scale, flaked off in places; blue underneath	Thin gray film on all surfaces, with scattered flakes of scale
ZO-13	6(K)		1.3146	0.9706	0.9362	−378.4	3.37	6.800	52.66	81.94	3.83	5.983	46.34	72.09				White powdery film with brown overlay in spots	Rough etched surfaces clean as defilmed, with chalky powder reforming in air
ZF-6	3(L)		1.3385	1.3556	1.3390	+0.5	3.37				3.83							Heavy rust-red scale, uniform over all surfaces	Thin blue film on all surfaces, with scattered flakes of scale
ZJ-12	4(L)		1.3674	1.3874	1.3687	+1.3	3.37				3.83							Heavy rust-red scale, uniform over all surfaces	Thin blue film on all surfaces, with scattered flakes of scale
ZM-12	5(L)		1.3359	1.3494	1.3362	+0.3	3.37				3.83							Heavy rust-red scale, uniform over all surfaces	Thin blue film on all surfaces, with scattered flakes of scale
ZP-14	6(L)		1.3452	1.3532	1.3456	+0.4	3.37				3.83							Heavy rust-red scale, uniform over all surfaces	Thin blue film on all surfaces, with scattered flakes of scale
ZT-3	1(M)		1.3846	1.4012	1.3890	+4.4	3.37				3.83							Heavy rust-red scale, uniform over all surfaces	Flakes of thin black scale retained on all surfaces
ZQ-3	3(M)		1.2904	1.3082	1.2908	+0.4	3.37				3.83							Heavy rust-red scale, uniform over all surfaces	Thin blue film on all surfaces, with scattered flakes of scale
ZR-3	4(M)		1.3687	1.3855	1.3705	+1.8	3.37				3.83							Heavy rust-red scale, uniform over all surfaces except on edge which is bare	Thin blue film on all surfaces
ZS-8	5(M)		1.3512	1.3707	1.3511	−0.1	3.37	0.002	0.15	0.24	3.83	0.002	0.02	0.02				Heavy rust-red scale, one side flaked off	Thin blue film on all surfaces, with flakes of scale retained around hole
ZU-4	8(M)		1.3702	1.3086	1.2893	−80.9	3.37	1.441	11.16	17.36	3.83	1.268	9.82	15.28				Heavy rust-red scale, flaked off in spots; powdery white underneath	Etched surfaces; clean on defilming, with chalky powder forming in air
V. 8 Pin Specimens (Zircaloy-3 and -4)																			
A. Core Pin Specimens																			
6 (Zr-3)			1.9583	1.9224	1.9205	−37.8	5.60	0.409	3.17	4.93	5.72	0.400	3.10	4.82	2.46	2.82	3.79	Light film with coloring from light blue to purplish; band of white film on one end	Thin gray film with metallic luster; all surfaces roughened
7 (Zr-3)			1.8807	1.7867	1.7863	−94.4	5.60	1.021	7.91	12.30	5.72	0.999	7.74	12.04	2.46	2.82	3.79	Light film with interference colors ranging from light blue to purple	Thin gray film with metallic luster; all surfaces roughened
8 (Zr-3)			1.9722	1.9321	1.9307	−41.5	5.60	0.449	3.48	5.41	5.72	0.440	3.41	5.30	2.46	2.82	3.79	Heavy black scale, uniform over all surfaces	Thin gray film with metallic luster; all surfaces roughened
9 (Zr-4)			2.0319	1.9391	1.9383	−93.6	5.60	1.012	7.84	12.19	5.72	0.991	7.67	11.94	2.46	2.82	3.79	Heavy black scale, uniform over all surfaces	Thin gray film with metallic luster; all surfaces roughened

*Two corrosion rates are presented: one based on the total operation time of 1128 hr and the other based on the total radiation time of 725 hr (3 Mwhr of reactor time equivalent to 1 hr of total radiation time).

Table 21 (continued)

Sample No.	Position	Flow Velocity (fps)	Weight Data: Initial (g)	Weight Data: As Removed (g)	Weight Data: Defilmed (g)	Weight Data: Change (mg)	Exposed Sample Area (cm^2)	Corrosion Penetration (mils)	Corrosion Rate* (Exposed Area) (mpy): 1128 hr	Corrosion Rate* (Exposed Area) (mpy): 725 hr	Total Area (cm^2)	Corrosion Penetration (mils)	Corrosion Rate* (Total Area) (mpy): 1128 hr	Corrosion Rate* (Total Area) (mpy): 725 hr	Distance from Front of First Specimen to Center of Specimen (in.)	Neutron Flux at Specimen Locations (neutrons·cm^{-2}·sec^{-1})	Power Density at Specimen Locations (w/ml)	Appearance: As Removed	Appearance: Defilmed
B. Line Pin Specimens																$\times 10^{12}$			
1 (Zr-3)			1.8792	1.8836	1.8796	+0.4	5.60				5.72							Light gray appearance; flakes of red scale scattered over all areas	Thin gray film with metallic luster; some scale retained on each end
2 (Zr-3)			1.9443	1.9464	1.9427	−1.6	5.60	0.017	0.13	0.20	5.72	0.017	0.13	0.20				Light gray appearance; flakes of red scale scattered over all areas	Thin gray film on etched surfaces
3 (Zr-3)			1.9484	1.9578	1.9391	−9.3	5.60	0.101	0.78	1.22	5.72	0.099	0.77	1.19				Light gray appearance; flakes of red scale scattered over all areas	Thin gray film on etched surfaces
4 (Zr-4)			1.9293	1.9682	1.9299	−0.6	5.60	0.006	0.05	0.07	5.72	0.006	0.05	0.07				Heavy red scale, flaked off in spots; light gray appearance underneath	Thin gray film with a metallic luster; some scale retained on each end
VI. Sapphire Specimens																			
L	Core		2.3505	2.3367	2.3359	−14.6	2.07	0.945	7.32	11.39	4.59	0.426	3.30	5.13	−0.5	6.20	8.33	Dark brown film over surface with patches of no film; bare places translucent	Translucent amber color; no scale retained
M	Core		2.3267	2.3117	2.3109	−15.8	2.07	1.021	7.91	12.30	4.59	0.460	3.56	5.54	−0.5	6.20	8.33	Dark brown film over surface with patches of no film; bare places translucent	Translucent amber color; no scale retained
VII. Core Coupon Holder #110 (Zircaloy-2)																			
Part A			74.2747**				86.5				95.3				3.0	2.57	3.45		
Part B			75.6682	75.4570	75.3650	−303.2	86.5	0.212	1.64	2.55	95.3	0.192	1.49	2.31	3.0	2.57	3.45	Thin holder was in the most part clean with scattered spots of scale	Thin gray film with a metallic luster; some scale retained in clamping band areas
VIII. In-Line Coupon Holder #111 (Zircaloy-2)																			
Part A			75.4929**				86.5				95.3								
Part B			75.3447	75.6391	74.2626	−1082.1	86.5	0.758	5.87	9.13	95.3	0.688	5.33	8.29				Heavy black scale, uniform over all surfaces	Some scattered scale retained; central region badly etched; ends smooth

*Two corrosion rates are presented: one based on the total operation time of 1128 hr and the other based on the total radiation time of 725 hr (3 Mwhr of reactor time equivalent to 1 hr of total radiation time).

**Damaged in disassembly.

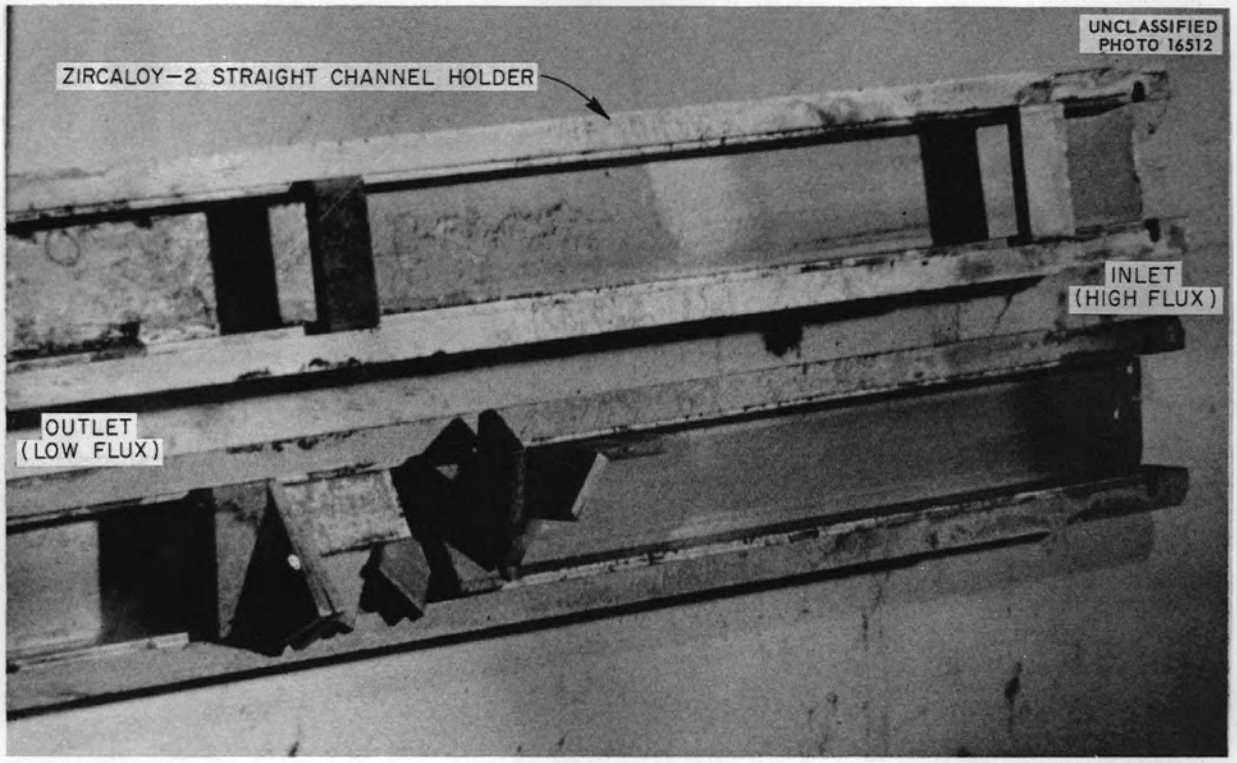

Fig. 16. Core Coupon Assembly After Exposure.

UNCLASSIFIED
PHOTO 16340

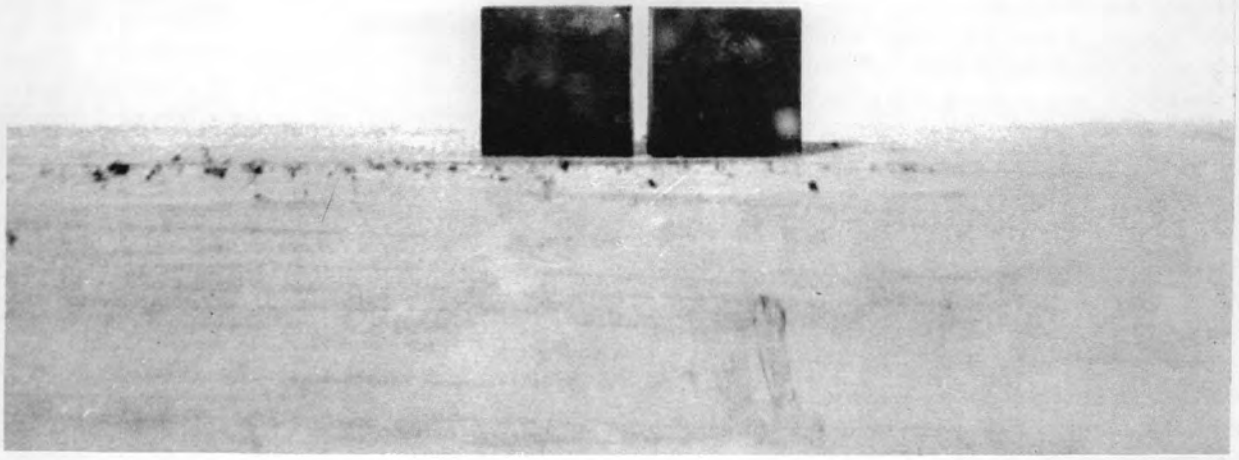

Fig. 17. Core Sapphire Specimens After Exposure.

flow rate of 3 cc/sec through sections of the pressurizer circuit were measured and compared with calculated pressure drops for the same sections. The drop through the entire circuit was measured first; then additional measurements were made following the removal of sections of the tubing from either end of the circuit. The pressure drop attributable to any section was thus obtained by difference. These measurements indicated that most of the flow reduction noted during operation of the loop was probably caused by an increased resistance to flow in the $\frac{1}{4}$-in. lines leading to and from the pressurizer and pressurizer heater. Visual examination failed to reveal a noticeable accumulation of foreign material in the tubing sections removed from the circuit.

Quantitative Inspection of Loop

Sample-weight data, together with other pertinent information, are presented in Table 21. Two different values for corrosion penetration were calculated for each specimen from the weight-change data. One value is based on the exposed area of the specimen, and the other is based on the total area. Two different corrosion-rate values are listed for each penetration value. One value was computed with total circulation time as a basis; the other was computed with radiation time as a basis. The value for the neutron flux to which a given core specimen was exposed during operation and the corresponding fission power density in solution are also listed in the table. The flux values are those which correspond to the specimen position in the core as shown by the flux vs position plot in Fig. 13. The values for the pin specimens and core coupon holder were obtained by averaging logarithmically the flux values at the ends of each. Table 22 lists the factors used in computing the amount of specimen corrosion penetration from weight losses. The materials represented by the various code numbers are given in Table 12.

This is the first loop experiment in which straight-channel coupon holders were used; hence no effect of velocity gradient on the core and in-line coupons could be observed. The solution velocity, which was initially 13.3 fps through the holders, is assumed to have increased to 17 fps when the pump speed was increased during the run, as previously mentioned. The corrosion-rate values summarized below were calculated from weight-loss data, with the exposed areas and total radiation time (equivalent to 725 hr of LITR operation at 3 Mw) used as the basis for the calculations.

Table 22. Corrosion Penetration Factors

Material	Density (g/cc)	Factor (mg of material/cm^2/mil penetration)
Platinum	21.45	54.48
Crystal-bar zirconium	6.5	16.51
Zircaloy-2	6.5	16.51
Zircaloy-3	6.5	16.51
Zircaloy-4	6.5	16.51
Zr–15% Nb	6.81	17.30
Zr–3% Nb	6.56	16.66
Al_2O_3	4.0	10.15
Sapphire	4.0	10.15
Stainless steel		
Type 347	8.02	20.37
Type 443	7.60	19.30
Type 446	7.60	19.30
Type 350A	7.79	19.79
Incoloy	8.51	21.61
Titanium	4.54	11.53

Zirconium and Zirconium Alloys. – The corrosion results obtained on Zircaloy-2 specimens were in good agreement with those obtained for Zircaloy-2 specimens in previous loops.[12] Rates observed varied from 2 mpy at 2 w/ml power density to 4 mpy at 6 w/ml power density. One of the striking results is that most of the other zirconium alloys tested corroded at about the same rate as Zircaloy-2 in the core region, with the same general power density dependency. The ZC, ZK, and ZL specimens corroded at roughly 2 to 3 times the Zircaloy-2 rates under similar conditions. The ZO coupons, zirconium with aluminum and manganese, corroded at rates of 59 to 121 mpy in the core region. The zirconium alloy pin-type specimens, rods I and III, corroded at a rate of about 5 mpy while rods II and IV corroded at a rate of 12 mpy. These pin

[12] J. E. Baker *et al.*, *HRP Radiation Corrosion Studies: In-Pile Loop L-4-8*, ORNL-2042 (Aug. 21, 1956).

specimens were at an average power density of 3.8 w/ml.

The ZT specimens, zirconium with 15% niobium, exhibited a negligible corrosion rate at 1.9 w/ml and a low rate of 1.2 mpy at 5.6 w/ml. The latter rate is less than one-third the rate observed for Zircaloy-2 at the same power density.

Most of the zirconium alloys in the in-line positions could not be defilmed completely, and weight gains were observed after the final defilming. Some of the exceptions were the ZO, ZC, and ZU specimens. In-line corrosion rates for the ZO specimens ranged from 59 to 82 mpy. Rates for the ZC coupons ranged from 3 to 5 mpy. The single ZU coupon corroded at a rate of 17 mpy. The in-line ZT specimen showed a weight gain of 2 to 3 times that of the Zircaloy-2 in-line specimens.

The Zircaloy-2 weld specimens and the Zircaloy-2 specimens with added H_2 did not appear to corrode at rates higher than those observed for Zircaloy-2.

All the zirconium alloy corrosion data from the core are shown in Fig. 18, where the logarithms of the corrosion rates of the specimens are plotted against the power density. The data in the shaded section are considered to be in good agreement with Zircaloy-2 data. The Zircaloy-2 corrosion data and other corrosion data in this shaded area are plotted against the power density in Fig. 19.

Titanium Alloys. – The average corrosion rates of titanium coupons in the core and in-line positions were 0.6 and 0.7 mpy, respectively. The corrosion rate of the holder coupons at a velocity of 13.3 fps was about 1 mpy as compared with an average of 0.4 mpy exhibited by the core rod coupons at a low velocity. Two of six Ti-75A in-line rod specimens exhibited corrosion rates of over 1 mpy as compared with a maximum rate of 0.4 mpy for a core rod coupon of this material.

Corrosion-rate values for the titanium alloy specimens in the core are plotted against the power density in Fig. 20.

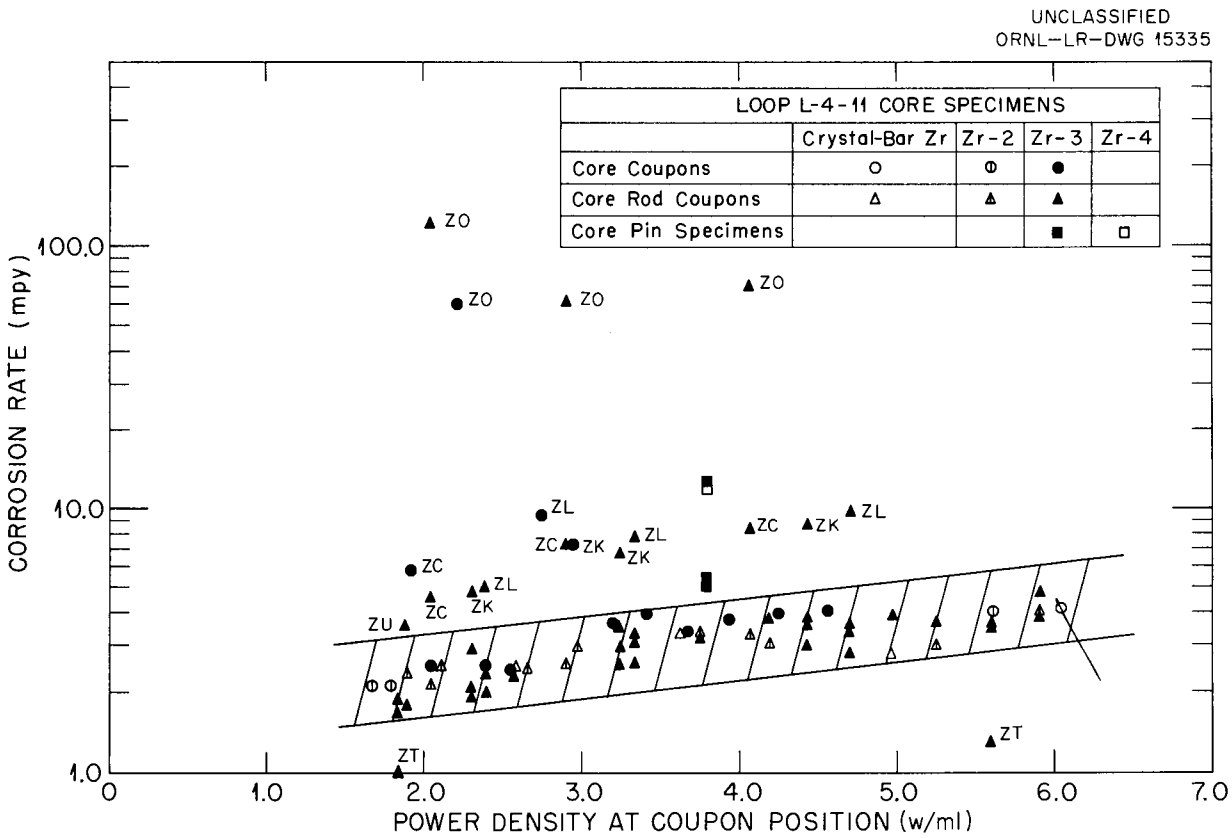

Fig. 18. Logarithm of Zirconium and Zirconium Alloy Specimen Corrosion Rates vs Power Density. The corrosion rates were calculated by using exposed areas and radiation time.

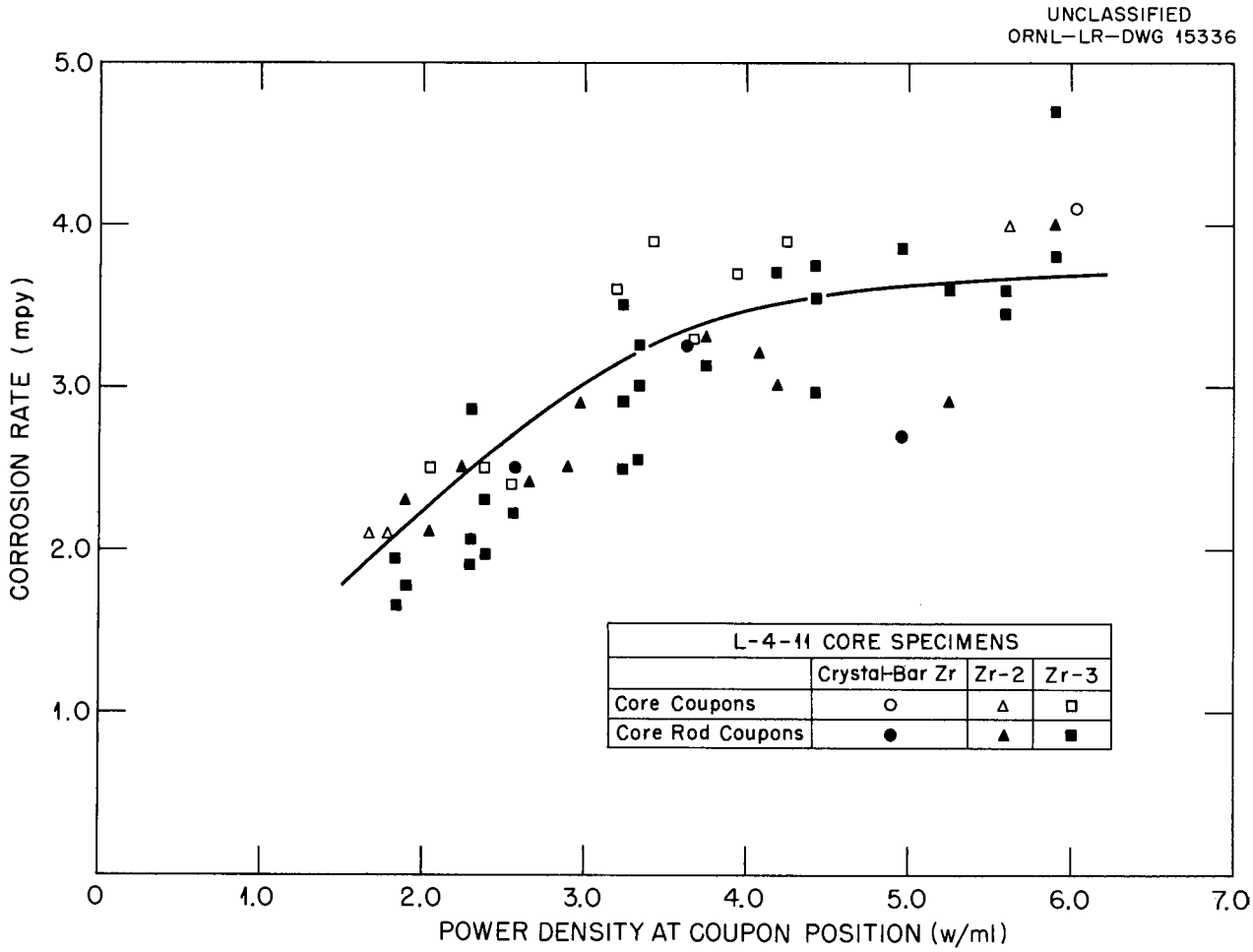

Fig. 19. Zirconium and Zirconium Alloy Specimen Corrosion Rates vs Power Density. The corrosion rates were calculated by using exposed areas and radiation time.

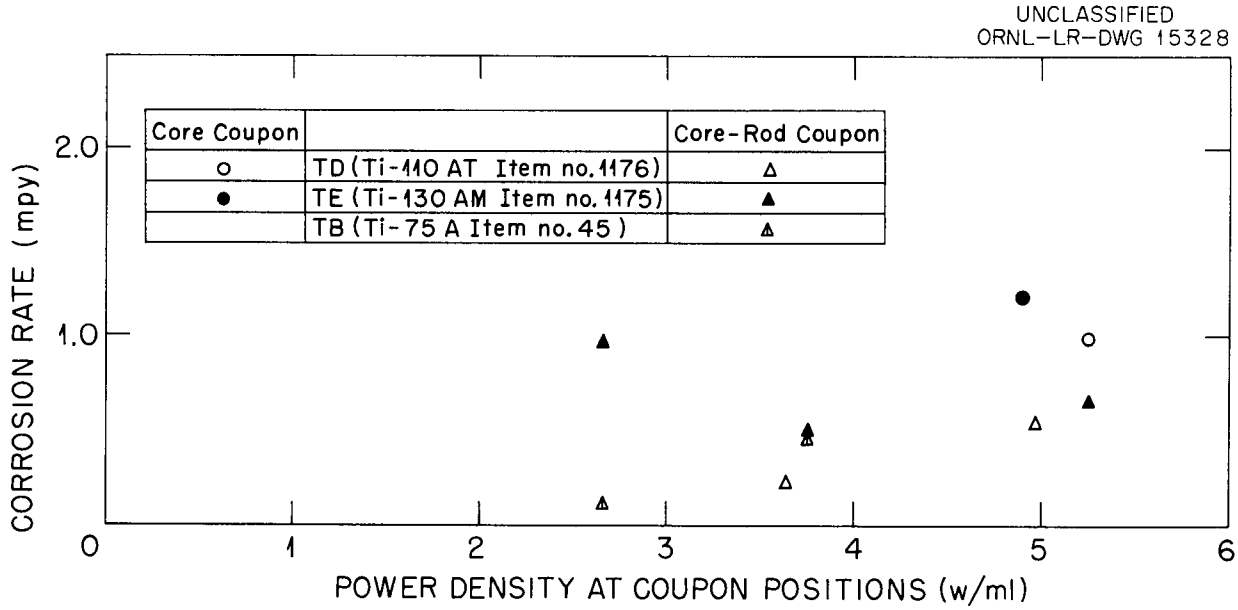

Fig. 20. Titanium Alloy Core Coupon and Core Rod Coupon Corrosion Rates vs Power Density. The corrosion rates were calculated by using exposed areas and radiation time.

Stainless Steel. – In Fig. 21, the corrosion rates of the stainless steel specimens in the core are plotted against the power density.

Only two stainless steel specimens were located in the core holder: one of type 347, the other of type 443. Both specimens were exposed at a power density of about 1.3 w/ml and at a solution velocity of 13 fps. The corrosion rate determined for each specimen was 2.2 mpy. This rate is approximately 1.3 times the rate observed for type 347 stainless steel under similar conditions in experiment L-4-8.

Core rod coupons of types 347, 350A, 443, and 446 stainless steel were exposed at power densities below 4 w/ml. The observed corrosion rate in each case is less than 1 mpy. One specimen of type 350A and one of type 446 stainless steel were exposed at higher power densities, about 5.5 w/ml. The observed rate for the type 350A is 2.2 mpy; that for the type 446 is 15.8 mpy.

The corrosion rate of the type 443 stainless steel coupon, which was located in the in-line holder, was about the same as that for the coupon in the core holder. However, the type 347 stainless steel coupon in the in-line holder had a corrosion rate of only 0.2 mpy.

The corrosion rates of the in-line rod coupons were inappreciable.

Incoloy. – The core coupon array contained one Incoloy specimen in the low flux region of the holder. The core rod coupon assembly contained three Incoloy specimens. With the exception of the core rod Incoloy specimen in the high flux region (4.2 w/ml), which had a high corrosion rate of 5.4 mpy, the corrosion rates were in general

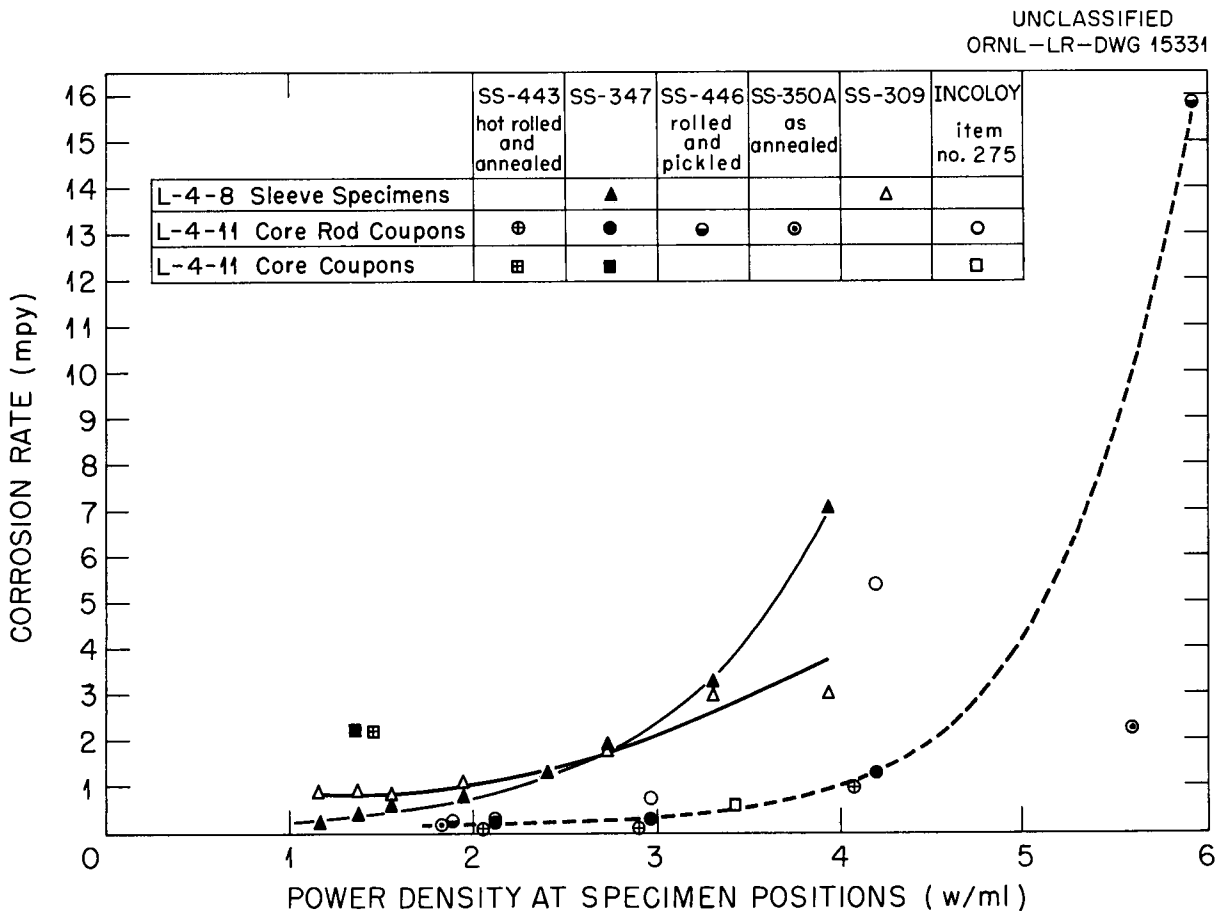

Fig. 21. Incoloy and Stainless Steel Core Specimen Rates vs Power Density. The corrosion rates were calculated by using exposed areas and radiation time.

agreement with the stainless steel core rod specimens at the same power densities. The in-line Incoloy specimens showed lower corrosion rates than the core specimens. Single specimens in the in-line holder and in-line rod arrays gave rates of 0.1 mpy each.

Platinum. – Platinum was found to corrode very slightly. Core coupons and core rod coupons gave corrosion rates of from 0.03 to 0.3 mpy. One coupon exhibited a rate of 1.6 mpy; however, this may have occurred as a result of damage to the specimen during removal from the loop. The in-line specimens showed either no weight change or a weight increase after the final defilming.

Sintered Alumina. – Two alumina specimens located in the core region and one in an in-line position disintegrated. A very small portion of the core rod coupon was in place after disassembly.

Synthetic Sapphire. – Two synthetic sapphires, which were held in a special bracket in front of the regular core specimen assemblies, acquired a loose, flaky deposit of transported iron oxides and lost much of their transparency. The power density in the sapphire location was about 8 w/ml and the corrosion rate of the specimens was about 12 mpy.

Metallographic Examination of Loop

Metallographic findings for this loop[13] and for previous loops[14–16] have been reported. As with the previous loops, various sections of the type 347 stainless steel components were examined. No evidence of localized attack was found in the sections from the piping at the pump outlet, the pressurizer heater, or the solution phase of the pressurizer. The vapor phase of the pressurizer again showed some slight penetration at the grain boundaries, as did the interior surface of the core cap. A section of this cap is shown in Fig. 22. Uniform attack of the various components cannot be estimated from metallographic examination because of the fabrication tolerances on the original stock.

Examination of one-half of the Zircaloy-2 coupon holder from the in-line position showed considerable surface roughening in the central region, with pitting depths up to 1 mil below the peaks, as shown in Fig. 23. There was some evidence of orientation of the attack, probably with reference to the rolling direction during fabrication. Similar

[13] A. E. Richt and J. O. Stiegler, *Metallographic Examination of Components and Coupons from HRP In-Pile Loop L-4-11*, ORNL CF-56-9-116 (Sept. 28, 1956).

[14] G. H. Jenks *et al.*, *HRP Quar. Prog. Rep. April 30, 1955*, ORNL-1895, p 94, esp 118–119.

[15] G. H. Jenks *et al.*, *HRP Quar. Prog. Rep. July 31, 1955*, ORNL-1943, p 105, esp 125–126 (classified).

[16] G. H. Jenks *et al.*, *HRP Quar. Prog. Rep. July 31, 1956*, ORNL-2148, p 92, esp 93 (classified).

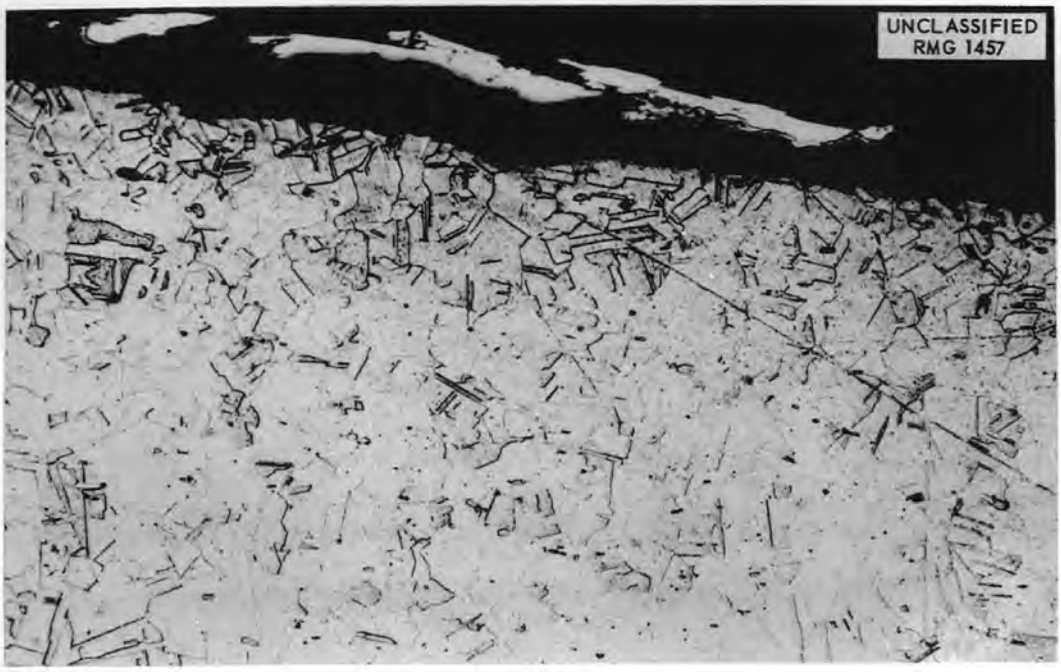

Fig. 22. Core Cap. 250X.

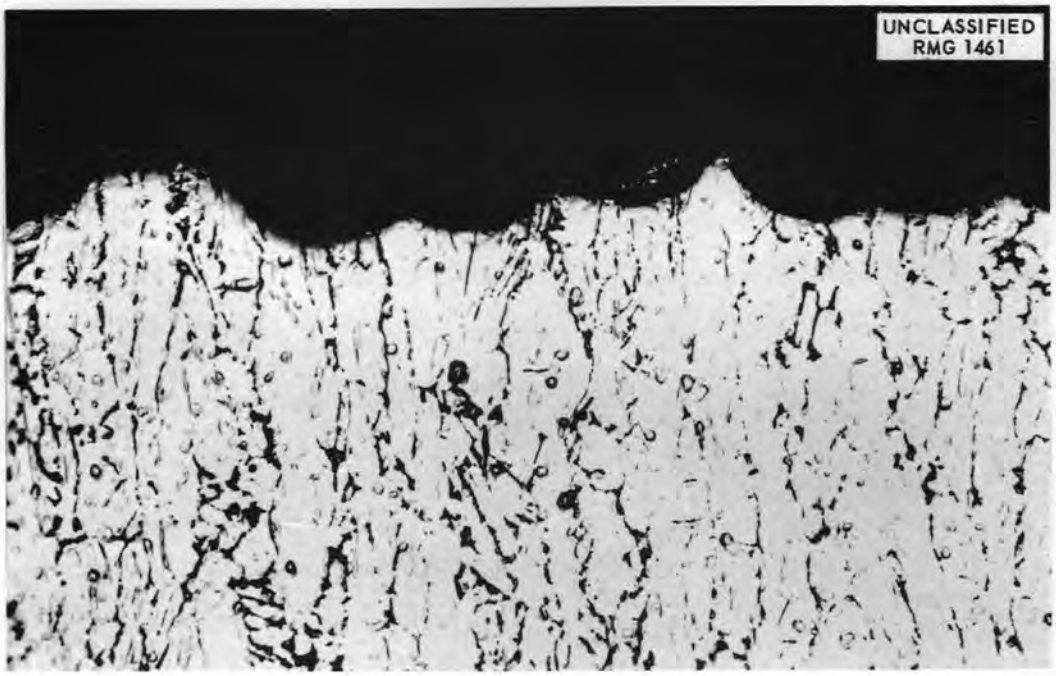

Fig. 23. Surface of In-Line Holder in Damaged Region. 250X.

microstructural areas have been seen by the HRP Metallurgy Group[17] and have been traced to macro segregation in the original ingot. Thus the increased attack may be a result of poor quality material and not a result of the exposure conditions.

The large variety of alloys included as specimens in this loop and the lack of adequate stock for pre-exposure comparison samples complicated the metallographic examination of the coupons. Consequently, only a limited number of alloys of unusual interest were selected. A review of the metallography by the HRP Metallurgy Group[17] reported no unusual microstructures that might be attributed to the radiation exposure. The surface condition of the specimens examined is summarized in Table 23.

DISCUSSION OF RESULTS

Correlation Between Nickel, Manganese, Oxygen, and Weight Data

The corrosion penetration values of the steel based on nickel, manganese, and oxygen data are plotted against circulation time in Fig. 10. Smooth curves through the nickel and manganese data are in good agreement with the oxygen data. The shapes of the curves for the period of operation with the original solution are of the same general type as those obtained for previous experiments, showing a high initial corrosion rate which decreases to a lower, fairly constant rate after the first few hundred hours. The curves for the period of operation following the second pretreatment operation and the charging of a fresh solution to the loop also display the same general shape as those for the first period of operation.

The over-all average corrosion penetration of steel based on nickel data was 0.35 mil. The corrosion penetration of the one type 347 stainless steel in-line specimen was 0.22 mil, which would indicate a corrosion rate of 0.2 mpy based on the circulation time. Assuming the remainder of the 2895 cm^2 steel surface outside the core corroded to this extent, then the average penetration of the 1066 cm^2 steel surface in the core would have been about 1.24 mils. This would indicate an average rate on the steel in the core of about 9.6 mpy. There were too few type 347 stainless steel specimens in the core to determine the average corrosion rate based on weight data.

As mentioned previously, it is assumed that oxygen is consumed only in the corrosion of steel in calculating the over-all corrosion rate shown in Fig. 10. Actually, a considerable quantity of

[17] M. L. Picklesimer, private communication to A. R. Olsen, January 1957.

Table 23. Summary of Results from Metallographic Examination of Coupons

Coupon No.	Exposure Position	Calculated Penetration (mils)	Surface Conditions
ZT	CR* 1(A)	0.1	Smooth, even; no evidence of corrosion attack
ZR	CR 11(E)	0.0	Smooth, even; no evidence of corrosion attack
ZT	ILR** 1(M)	Wt gain	Smooth, even; no evidence of corrosion attack
ZU	CR 1(H)	0.4	Slight surface roughening; approximately ½ mil penetration
ZU	ILR 8(M)	1.4	Slight surface roughening; approximately ½ mil penetration; ends heavily attacked
ZD-8	CR 5(G)	0.3	Smooth, undulating surface; no localized attack
ZE-6	CR 2(H)	0.3	Smooth, undulating surface; no localized attack
ZK-12	CR 3(E)	0.7	Smooth, undulating surface; no localized attack
ZO-11	CR 4(A)	5.7	Very rough, uneven surface; heavy surface film or scale
ZO-13	ILR 6(K)	6.8	Very rough, uneven surface; heavy surface film or scale
IN-12	CR 4(F)	0.4	Slight surface roughening, approximately ½ mil deep
IN-14	ILR 8(J)	0.01	Smooth, undulating surface; no localized attack
TB-1481A	CR 5(B)	0.04	Smooth, even surface; no evidence of corrosion attack
TB-1478A	ILR 9(J)	0.01	Smooth surface; slightly undulating surface
TB-1475A I	ILR 9(K)	0.13	Smooth, even surface; no evidence of corrosion attack

*CR 1(A): core rod A, position 1
**ILR 1(M): in-line rod M, position 1

the oxygen was consumed in the oxidation of other metals. If the oxygen consumed in the oxidation of metals other than steel (primarily zirconium alloys) is considered, the over-all rate for steel is about 18% lower. The average steel corrosion penetration based on corrected oxygen data would be 0.28 mil, which would indicate an over-all rate of 2.2 mpy.

Correlation Between Excess Acid and Over-All Rate

The initial excess acid was over 0.04 *m*; however, as shown in Fig. 12, the nickel and manganese produced in the corrosion of the steel reduced the excess acid to less than 0.03 *m* in less than 200 hr. The corrosion rate during irradiation after this time appears to be considerably less than that when the acid was higher. A similar effect was noted in experiments FF (ref 18), GG (ref 19), and L-4-8 (ref 20). Operating conditions of these experiments are listed in Table 20.

[18] G. H. Jenks *et al.*, *HRP Quar. Prog. Rep. April 30, 1955*, ORNL-1895, p 99–118.

[19] G. H. Jenks *et al.*, *HRP Quar. Prog. Rep. July 31, 1955*, ORNL-1943, p 109–125 (classified).

[20] J. E. Baker *et al.*, *HRP Radiation Corrosion Studies: In-Pile Loop L-4-8*, ORNL-2042 (Aug. 21, 1956).

Quantitative Weight Data

Only one of the many zirconium alloys tested exhibited corrosion rates appreciably lower than Zircaloy-2. That alloy, zirconium with 15% niobium, corroded at a rate less than one-third the rate observed for Zircaloy-2 at the same power density.

The corrosion rates of most of the zirconium alloys and crystal-bar zirconium were in agreement with Zircaloy-2 data; however, a few alloys corroded at considerably higher rates. For instance, the ZO coupons, zirconium with aluminum and manganese, corroded at rates over 20 times those observed for Zircaloy-2 at the same power density. The in-line rate on these specimens was also very high, over 50 mpy.

In a previous discussion of Zircaloy-2 in-pile corrosion data[21] the relationship between corrosion rate and power density over the range studied was shown to be expressed by equations of the general form:

$$(CR) = A(PD)\left(1 - e^{-B/CR^{1.5}}\right) ,$$

where

CR = corrosion rate in mpy,

PD = power density in w/ml,

A = constant depending on solution composition and temperature,

B = constant depending on temperature.

Values for the constants A and B were previously established as 1.25 and 8.3, respectively, from in-pile autoclave and loop experiments conducted at 250°C and utilizing 0.17 m UO_2SO_4 solutions. These data plus more recent autoclave data were re-evaluated, and the resulting constants A and B are 1.25 and 6.5, respectively. The corrosion data on Zircaloy-2 in this experiment are expressed reasonably well by the above equations using the latter constants.

The corrosion rates observed on titanium alloy specimens were in the range of those observed on such alloys in out-of-pile experiments. There was little difference between the average core and in-line rates. The experiment contained no titanium 55AX; however, the rates on the in-line titanium specimens (types 75A, 110AT, and 130AM) were higher than those observed on titanium 55AX in previous experiments.[19]

Solution Stability

No evidence of solution instability was noted during this experiment. The corrected uranium and copper concentrations remained near their initial values throughout the run. The indication by analytical results that more uranium was recovered in the weigh tank than was originally charged to the loop is additional evidence that the uranium was in solution when the loop was drained.

Metallographic Results

The metallographic results are summarized in Table 23. In general, these observations confirm the macro surface examination findings and show further that the type of attack was not highly localized on any of the materials examined. For example, it is felt that the undulations in Fig. 24 of titanium coupon TB-1478A are the remains of the original machine marks. There were three bands of highly twinned structure on TB-1475A, as shown in Fig. 25. The worked condition of this sample may account for the relatively high penetration as calculated from weight-loss measurements, but there is no indication of surface depression in the region of twinning. It appears, to date, that differences in the success of the defilming operation in removing the thin adherent titanium oxide account for the variations between samples from a given loop.

---

[21] G. H. Jenks *et al.*, *HRP Quar. Prog. Rep. Oct. 31, 1956*, ORNL-2222, p 100, esp 111.

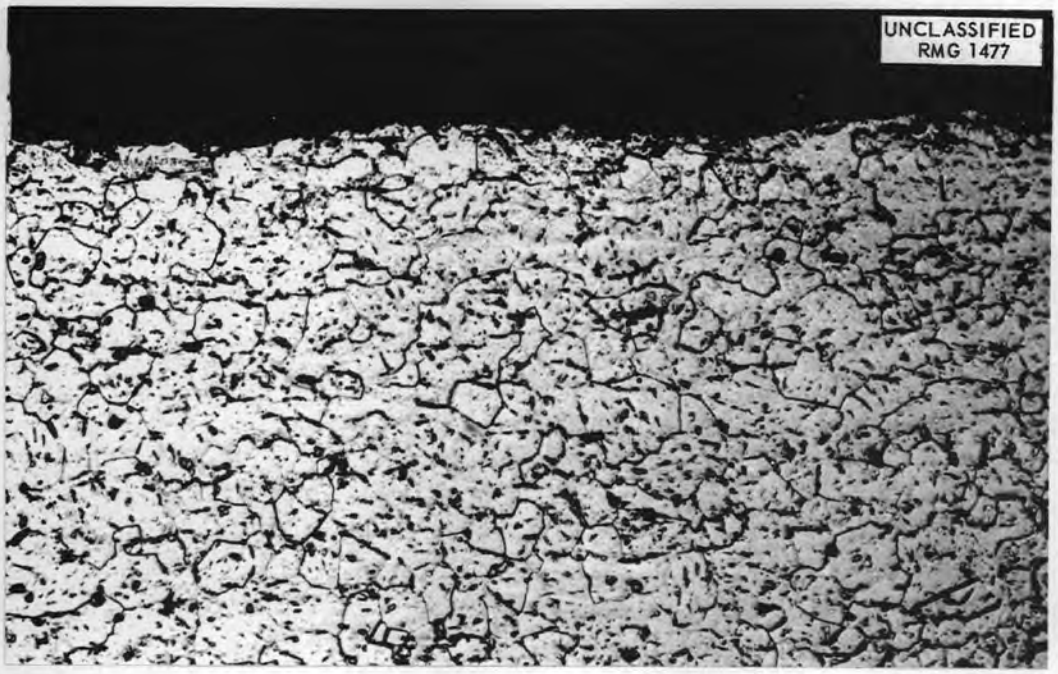

Fig. 24. Coupon TB-1478A. 250X.

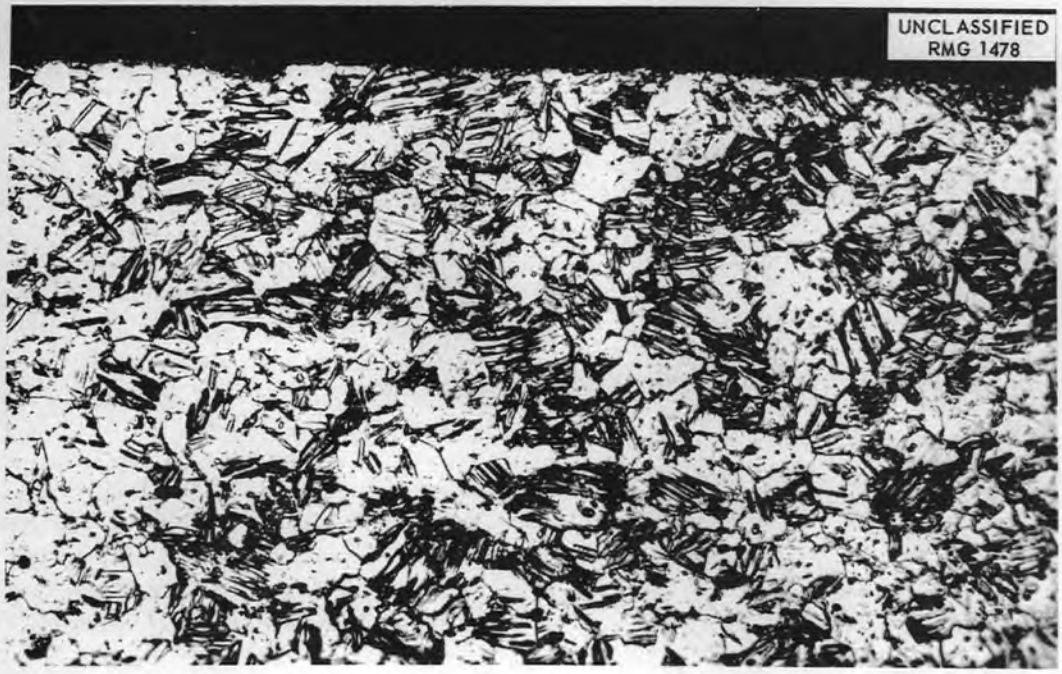

Fig. 25. Twinned Area of Coupon TB-1475A. 250X.

INTERNAL DISTRIBUTION

1. C. E. Center
2. Biology Library
3. Health Physics Library
4. Metallurgy Library
5. Reactor Experimental Engineering Library
6. Central Research Library
7–26. Laboratory Records Department
27. Laboratory Records, ORNL R.C.
28. G. M. Adamson
29. A. L. Bacarella
30. J. E. Baker
31. S. E. Beall
32. A. M. Billings
33. D. S. Billington
34. E. P. Blizard
35. E. G. Bohlmann
36. S. E. Bolt
37. C. J. Borkowski
38. G. E. Boyd
39. N. C. Bradley
40. J. C. Bresee
41. J. W. Brown
42. F. R. Bruce
43. W. D. Burch
44. C. A. Burchsted
45. A. D. Callihan
46. D. W. Cardwell
47. W. L. Carter
48. G. H. Cartledge
49. R. A. Charpie
50. R. D. Cheverton
51. H. C. Claiborne
52. W. E. Clark
53. T. E. Cole
54. E. L. Compere
55. F. L. Culler
56. J. S. Culver
57. R. J. Davis
58. V. A. DeCarlo
59. J. S. Drury
60. J. L. English
61. W. K. Eister
62. L. B. Emlet (K-25)
63. D. E. Ferguson
64. J. H. Frye, Jr.
65. C. H. Gabbard
66. J. L. Gabbard
67. W. R. Gall
68. H. E. Goeller
69. R. S. Greeley
70. A. T. Gresky
71. J. C. Griess
72. E. Guth
73. P. A. Haas
74. P. H. Harley
75. P. N. Haubenreich
76. J. W. Hill
77. A. Hollaender
78. A. S. Householder
79. G. H. Jenks
80. D. T. Jones
81. W. H. Jordan
82. S. I. Kaplan
83. P. R. Kasten
84. C. P. Keim
85. M. T. Kelley
86. R. B. Korsmeyer
87. K. A. Kraus
88. J. A. Lane
89. R. E. Leuze
90. S. C. Lind
91. R. B. Lindauer
92. R. S. Livingston
93. R. A. Lorenz
94. M. I. Lundin
95. R. N. Lyon
96. J. L. March (C&CCC, South Charleston)
97. W. L. Marshall
98. H. F. McDuffie
99. J. P. McBride
100. H. A. McLain
101. R. A. McNees
102. J. R. McWherter
103. O. Menis
104. E. C. Miller
105. C. S. Morgan
106. K. Z. Morgan
107. J. P. Murray (Y-12)
108. M. L. Nelson
109. A. R. Olsen

110. L. F. Parsly
112. Sigfred Peterson
113. D. Phillips
114. M. L. Picklesimer
115. L. R. Quarles
116. S. A. Reed
117. P. M. Reyling
118. D. M. Richardson
119. R. C. Robertson
120. A. M. Rom
121. M. W. Rosenthal
122. H. C. Savage
123. C. L. Segaser
124. E. D. Shipley
125. M. D. Silverman
126. M. J. Skinner
127. A. H. Snell
128. I. Spiewak
129. R. W. Stoughton
130. C. D. Susano
131. J. A. Swartout
132. E. H. Taylor
133. D. G. Thomas
134. P. F. Thomason
135. M. Tobias
136. D. S. Toomb
137. W. E. Unger
138. R. Van Winkle
139. F. J. Walter
140. R. M. Warner
141. B. Weaver
142. A. M. Weinberg
143. S. H. Wheeler
144. E. P. Wigner (consultant)
145. G. C. Williams
146. C. E. Winters
147. W. C. Yee
148. F. C. Zapp
149. ORNL-Y-12 Technical Library, Document Reference Section
150. HRP Director's Office

EXTERNAL DISTRIBUTION

151. Division of Research and Development, AEC, ORO
152–737. Given distribution as shown in TID-4500 (13th ed., Rev., Feb. 15, 1958) under Reactors – General Category (75 copies – OTS)